Textile Science & Research Journal
ISSN: 3059-846X Volume – 1, Issue – 1, 2025
DOI: https://doi.org/10.63456/tsrj-1-1-31

PROCESSING AND CHARACTERIZATION OF CONDUCTIVE POLYETHER ETHER KETONE/CARBON NANOTUBE MONOFILAMENTS AND CORE–SHEATH FILAMENTS

TOTY ONGGAR[1*], LEOPOLD ALEXANDER FRANKENBACH[1] AND CHOKRI CHERIF[1]

Institute of Textile Machinery and High-Performance Material Technology (ITM), Technical University Dresden, 01062 Dresden, Germany

TOTY ONGGAR: toty.onggar@tu-dresden.de
LEOPOLD ALEXANDER FRANKENBACH: leopold_alexander.frankenbach@tu-dresden.de
CHOKRI CHERIF: chokri.cherif@tu-dresden.de

Corresponding Author: TOTY ONGGAR

ABSTRACT

The increasing demand for lightweight, high-performance materials has driven the development of textile-reinforced composites with integrated sensing capabilities. While thermoset-based composites have established sensor integration strategies, thermoplastic composites face challenges due to high processing temperatures. This study presents a novel approach to produce high-temperature-resistant, electrically conductive polyether ether ketone with multi-walled carbon nanotubes (PEEK/MWCNT) monofilament and core-sheath (PEEK-MWCNT/PEEK) filament yarns suitable for textile processing and structural health monitoring. Filaments were produced using a twin-screw extrusion site and a bicomponent melt spinning plant, systematically varying MWCNT content (1.0–7.0 wt.%) and process parameters. Differential scanning calorimetry revealed that MWCNTs influence PEEK crystallinity, glass transition temperature, and thermal transitions, while scanning electron microscopy (SEM) images confirmed filler dispersion and morphology. Mechanical testing demonstrated increased stiffness and tensile strength with higher MWCNT loading, while elongation at break decreased. Integration of conductive filaments into glass fiber/polypropylene (GF/PP) composites maintained or slightly improved composite mechanical properties. Electrical contacting via crimping combined with conductive epoxy provided stable, low-resistance connections. The results demonstrate that PEEK/MWCNT sensor yarns are suitable for high-temperature, textile-reinforced thermoplastic composites, offering a robust platform for intrinsically conductive, processable, and mechanically stable structural health monitoring systems.

KEYWORDS: Poly ether ether ketone, carbon nano tubes, sensor yarn, electrical conductivity, mechanical properties, thermoplastic composite

1. INTRODUCTION

The growing demands for energy and resource efficiency, along with global efforts to reduce CO_2 emissions, have driven the development of innovative lightweight materials. Textile-reinforced composites (TRCs) have attracted increasing attention due to their excellent specific stiffness and strength, combined with additional advantages, such as corrosion resistance, impact toughness, and fatigue durability. [1,2] These materials are widely used in high-performance applications, including aerospace, [3,4] marine engineering, [5] defense, [6,7] transportation, [8,9] and renewable energy sectors such as wind turbine construction. [10,11]

In recent years, the integration of sensing functionalities into composite materials has become increasingly important for structural health monitoring and real-time performance evaluation. While various strategies have been established for thermoset-based composites, sensor integration into thermoplastic matrix composites remains challenging due to high melt temperatures. Carbon fibers (CF) are often employed as sensing yarns because of their electrical conductivity, thermal stability, and mechanical robustness. [12–14] However, their low strain-to-failure (0.8– 1.54%) and high stiffness restrict their sensing range. [15,16] Alternative solutions using metallized polyamide yarns are limited by insufficient thermal stability or poor compatibility with textile processing, [17] while metallic wires lack flexibility and processability. [18]

To address these limitations, conductive polymer nanocomposites (CPNCs) have emerged as promising materials that combine the flexibility of polymers with the electrical properties of conductive fillers such as carbon nanotubes (CNTs). Most studies to date have focused on low-temperature thermoplastics, including polypropylene (PP, $T_m \approx 165 \pm 10°C$), polyamide (PA, $T_m \approx$

220–260°C, depending on the PA type), polycarbonate (PC, $T_m \approx 230$°C), and polyethylene terephthalate (PET, $T_m \approx 250 \pm 10$°C). Although, these polymers are suitable for low to medium temperature applications, their limited thermal resistance constrains their use in high-performance thermoplastic composite systems. Furthermore, previous research has largely concentrated on molded or film samples rather than textile-processable fibers and yarns, which are essential for integrating sensing functionalities into textile structures.

The use of high-performance thermoplastics such as poly ether ether ketone (PEEK) as a matrix material for conductive fibers or sensor yarns has been explored only in limited studies, mainly due to the challenges associated with CNT dispersion and processing at elevated temperatures. PEEK is a semi-crystalline, high-performance thermoplastic with exceptional thermal stability (up to 340°C), high mechanical strength (elastic modulus 3.6–4.1 GPa, tensile strength 90–100 MPa), and significant elongation at break (16–80%), making it a suitable candidate for advanced thermoplastic composite applications. [16, 19–21]

This study presents a novel approach to develop a high-temperature-resistant, electrically conductive sensor yarn based on a PEEK/MWCNT nanocomposite. By optimizing the filler content near the percolation threshold, a stable conductive network can be achieved, ensuring reliable electrical performance even under mechanical deformation. The proposed PEEK/MWCNT sensor yarn offers a new route toward intrinsically conductive, thermally stable, and textileprocessable sensing elements for next-generation thermoplastic composites with integrated monitoring capabilities.

EXPERIMENTAL PART

MATERIALS

The high purity PEEK VICTREX™ PEEK polymer 151G, manufactured by VICTREX PLC (Lancashire, UK), was used in the present research. PEEK is an unfilled, unreinforced and easy flowing, semi-crystalline, thermoplastic polymer with a density of 1.3 g/cm³, which is in the form of granules. A masterbatch from the manufacturer LEHMANN & VOSS CO. (Hamburg, Germany) with the designation LUVOCOM 1105®-8199 was used to generate the extrinsic electrical conductivity. LUVOCOM 1105®-8199 is a PEEK with 7 wt.% MWCNT and a density of 1.33 g/cm³ according to DIN ISO 1183-3 [22] and a surface resistance of $<10^6$ Ohm according to DIN EN 62631-3-2. [23]

A two-layer biaxial scrim made of E-CR glass fiber (GF) with polypropylene (PP) with a mass per unit area of 1045 ± 5 g/m² was used to produce the thermoplastic composite panels. This was manufactured by P-D GLASSEIDEN GMBH (Oschatz, Germany). The first layer is characterized by a 90° orientation and has a mass per unit area of 590 g/m² and a fineness of 1,870tex. The second layer is 0°-oriented and has a mass per unit area of 442 g/m² and a fineness of 1870 tex.

Production of high-temperature resistant, electrically conductive PEEK filament yarns Production of PEEK-MWCNT monofilament yarns

To produce PEEK-MWCNT monofilament yarns, the polymer Victrex™ PEEK 151G**,** the masterbatch LUVOCOM 1105®-8199 and the corresponding PEEK-MWCNT compound were first dried in a drying oven at 150°C for five hours until a moisture content of 0.05% was reached. In a subsequent step, PEEK-MWCNT monofilament yarns were produced using a ZSE 18 MAXX 40D twin-screw extruder (LEISTRITZ, Nuremberg, Germany). The dried pellets— composed of PEEK 151G and LUVOCOM 1105®-8199 masterbatch—were blended in the feed hopper and then fed into the extruder (Figure 1). The first feed zone was heated to 50°C, while the remaining eight heating zones were set to 380°C. The extruder was equipped with a 20 mm screw with a length of 0.8 m. A constant throughput of 0.6 kg/h was maintained, corresponding to a calculated shear rate of 161 s^{-1} (density: 1.32 g/cm³), and the screw speed was set to 50 rpm. The molten PEEK-MWCNT mixture was extruded through a die, solidified in a cooling section, and subsequently wound onto spools. In total, seven PEEK-MWCNT monofilament yarns with varying MWCNT contents were produced, along with a pure PEEK monofilament used as a reference (Table 1).

Textile Science & Research Journal
ISSN:3059-846X Volume – 1, Issue – 1, 2025
DOI: https://doi.org/10.63456/tsrj-1-1-31

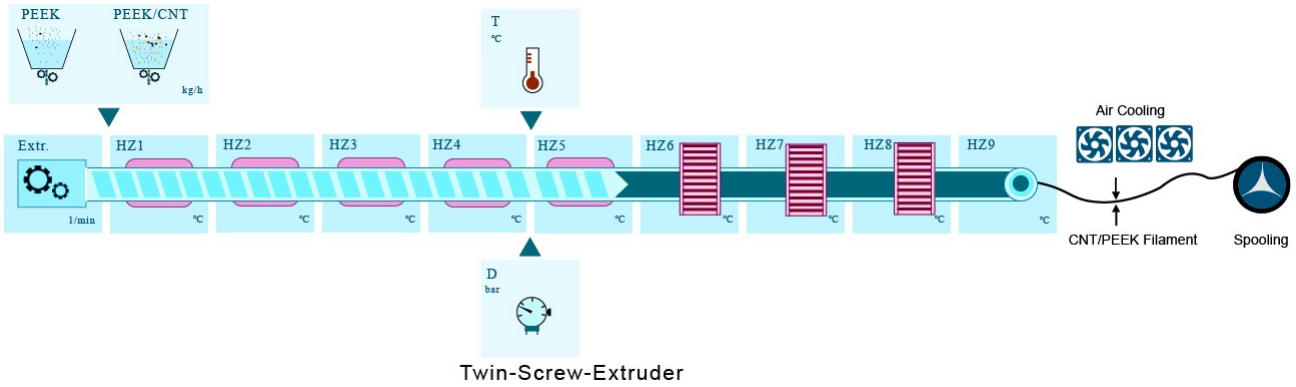

Figure 1. Twin-screw extruder (TSE) ZSE 18 MAXX 40D from a bicomponent melt spinning line for the compounding and extrusion a mixture of pure PEEK and PEEK-MWCNT masterbatches.

Some of the spun monofilaments were shredded and reused as compound material in a bicomponent melt-spinning process to create electrically conductive PEEK-MWCNT filaments. Before being re-melt-spun, the shredded yarns were subjected to further analyses, including viscosity and flow behavior, phase transitions, and chemical structure characterization. All produced PEEK and PEEK-MWCNT monofilaments were then evaluated for their mechanical and electrical properties.

Table 1. Overview of the PEEK-MWCNT monofilament yarns produced on the basis of different MWCNT contents using the TSE ZSE 18 MAXX 40D

Sample No	Smaple Name	Compound		MWCMT (wt.%)
		PEEK	Masterbatch	
1	PEEK	Victrex™PEEK	none	0.0
2	PEEK-MWCNT (7.0 wt.%)	none	LUVOCOM 1105 -8199®	7.0
3	PEEK-MWCNT (6.0 wt.%)	Victrex™PEEK	LUVOCOM 1105 -8199®	6.0
4	PEEK-MWCNT (5.0 wt.%)	Victrex™PEEK	LUVOCOM 1105 -8199®	5.0
5	PEEK-MWCNT (3.5 wt.%)	Victrex™PEEK	LUVOCOM 1105 -8199®	3.5
6	PEEK-MWCNT (2.0 wt.%)	Victrex™PEEK	LUVOCOM 1105 -8199®	2.0
7	PEEK-MWCNT (1.0 wt.%)	Victrex™PEEK	LUVOCOM 1105 -8199®	1.0

PRODUCTION OF CORE-SHEATH (C-S) FILAMENT YARNS (CORE: PEEK/MWCNT AND SHEATH: PURE PEEK)

A bicomponent melt spinning system was used to produce electrically conductive core-sheath (C-S) filament yarns. The core consisted of a PEEK-MWCNT mixture with 0.5 wt.% MWCNT content, which was processed using a twin-screw extruder (TSE) ZSE 18 MAXX 40D. The Sheath made of pure PEEK 151G was extruded using a single-screw extruder (SSE). The extruder temperatures in the core area increased zone by zone from 80°C to 380°C, in the sheath area from 360°C to 400°C. The speed of the TSE was a constant 5 rpm. For the SSE, the speed was initially set to 5 rpm in three tests and then to 10 rpm in a further three tests. The spinneret had a diameter of 1.6 mm for the core and 2.8 mm for the sheath, with a constant spinneret temperature of 400°C. The draw-off speed of the filament was varied between 90 m/min and 140 m/min to achieve the desired C-S structure (Table 2). The produced C-S filament yarns (PEEKMWCNT/PEEK) were also used for further thermal, mechanical and electrical investigations.

Textile Science & Research Journal
ISSN: 3059-846X Volume – 1, Issue – 1, 2025
DOI: https://doi.org/10.63456/tsrj-1-1-31

Table 2. Melt spun C-S filament yarns made from PEEK-MWCNT as core and PEEK as sheath as a function of the increasing draw-off speed and speed of the SSE

Sample No	Core-sheath filament yarn	Speed (rpm)		Pull-off speed (m/min)
		TSE	SSE	
1	Core (PEEK-MWCNT (0.5 wt.%) Sheath (PEEK)	5	5	9
2				100
3				110
4		5	10	110
5				120
6				140

CONTACTING

In order to integrate the melt-spun monofilament yarn (PEEK-MWCNT) and C-S filament yarn (PEEKMWCNT/PEEK) as sensor yarn in thermoplastic textile fiber-reinforced composite material, the filament yarns were first contacted. Two methods were compared to produce the electrical connection in order to determine which had the lowest electrical resistance: Firstly, a pure crimp connection, and secondly, a combination of crimping and conductive CHEMICALS COLD SOLDER 2K epoxy adhesive (Landshut, Germany).

INTEGRATION OF THE SENSOR YARNS IN THERMOPLASTIC COMPOSITES

The thermoplastic composite sheets with integrated monofilament yarn (PEEK-MWCNT) and C-S filament yarn (PEEK-MWCNT/PEEK) as sensor yarns were manufactured by means of a combined pressure and temperature process using a laboratory hot press (MODEL P300 PV, DR. COLLIN GMBH, Maitenbeth, Germany). The plate dimensions were 274 × 274 mm². The sensor yarns were integrated by positioning them in a 0° direction between two layers of a GF and PP biaxial fabric. The sensor yarns were fixed and tensioned between the bonding yarns of the scrim to ensure a straight yarn path (Figure 2).

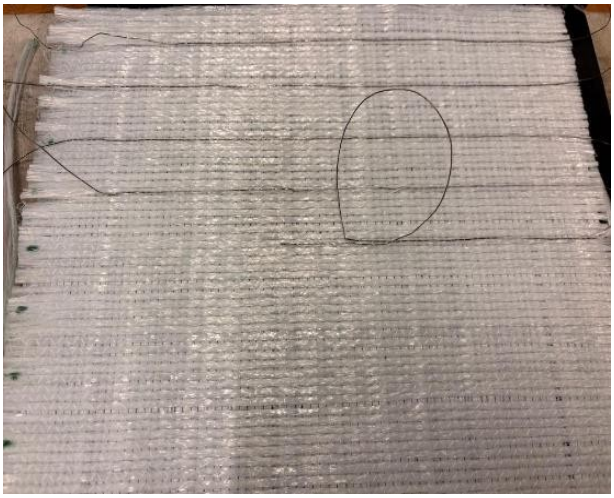

Figure 2. Fixation of the electrically conductive PEEK-MWCNT monofilament yarn with bonding threads to the GF/PP fabrics.

This procedure enabled uniform impregnation of the yarn structures with the PP matrix during the subsequent consolidation process. The thermal consolidation of the GF/PP biaxial fabric with integrated sensor yarn was carried out in the laboratory hot press under a defined linear temperature profile. The temperature was increased to 180°C at a controlled heating rate in order to completely melt the PP matrix material and ensure effective wetting of both the glass fibers and the PEEK-MWCNT sensor yarns. Parallel to the temperature increase, a specific forming pressure of 57.5 bar was applied. After reaching the final temperature, this was kept constant for a holding time of 30 min. This ensured complete infiltration of the fiber structures by the matrix, minimized air inclusions and ensured homogeneous consolidation. After completion of the holding phase, controlled cooling to room temperature (RT) took place, with the pressure being maintained continuously. The embedded sensor yarns remained functional and mechanically stable in the GF/PP composite during the entire process. The composite plates produced in this way were subsequently used for mechanical and electrical characterization.

Textile Science & Research Journal
ISSN: 3059-846X Volume – 1, Issue – 1, 2025
DOI: https://doi.org/10.63456/tsrj-1-1-31

ANALYSIS

DETERMINATION OF THE FILAMENT DIAMETER USING LIGHT MICROSCOPY

To determine the diameter of the manufactured electrically conductive monofilament (PEEK-MWCNT) and C-S filament yarns (PEEK-MWCNT/PEEK), they were first embedded in epoxy resin. The samples were then ground with a grinder and cleaned with ethanol. The diameter of the filament yarns was then measured at several points using the AXIO Imager.M1m optical microscope from CARL ZEISS MICROSCOPY DEUTSCHLAND GMBH (Oberkochen, Germany) and the mean value was calculated.

DETERMINATION OF MASS CHANGES USING THERMOGRAVIMETRY (TGA)

In the present study, the thermal stability and decomposition temperatures of pure PEEK, the masterbatch and PEEKMWCNT mixture with a weight of 12−14 mg were carried out with the Thermogravimetry TGA Q500 from TA Instruments (Eschborn, Germany) at a heating rate of 10 K/min and a temperature range of 30−800°C under oxidative (air) and inert (nitrogen) atmosphere.

DETERMINATION OF PHASE TRANSITIONS USING DIFFERENTIAL SCANNING CALORIMETRY (DSC)

The determination of material properties and phase transitions, such as melting point, glass transition temperature, crystallization and melting temperature over time and degree was performed using Differential Scanning Calorimetry DSC Q2000 from TA Instruments (Eschborn, Germany) according to the standards of ASTM D3418-15 [24] using pure PEEK, masterbatch and its blends with a weight of 10−12 mg. The samples were subjected to thermal analysis by heating from 50−400°C at a heating rate of 10 K/min, followed by rapid cooling from 400−50°C and reheating to 400°C (second heating cycle). It should be noted that all analysis steps were carried out in a nitrogen atmosphere. The data was used for the analysis.

SURFACE MORPHOLOGY AND MWCNT DISPERSION CHARACTERIZATION BY SCANNING ELECTRON MICROSCOPY (SEM)

To evaluate the dispersion and agglomeration behavior of MWCNTs as well as the morphology of the extruded PEEK/MWCNT filament yarns, scanning electron microscopy (SEM) was performed. Cross-sections of the filaments with varying MWCNT contents (1–7 wt.%) were prepared and analyzed using a DSM 982 Gemini (CARL ZEISS AG, Jena, Germany). SEM imaging at magnifications of 100× enabled a qualitative assessment of the nanotube distribution within the PEEK matrix and the identification of agglomerates and their size distribution.

MECHANICAL CHARACTERIZATION TENSILE TEST ON FILAMENT YARNS

Prior to the mechanical tests, all filament yarns were conditioned for 24 hours under standard climatic conditions in accordance with DIN EN ISO 139. The tensile tests to determine the maximum tensile force and the associated elongation were carried out in accordance with DIN EN ISO 2062 using a universal testing machine (ZMART.PRO, ZWICK GMBH & CO. KG, ULM, GERMANY) with a nominal load of 10 kN. The filament yarns were fixed with steel clamping jaws (type 8253, 30 mm × 30 mm).

In addition, the temperature resistance of the PEEK-MWCNT monofilament yarns was investigated with regard to their use in thermoplastic composites. For this purpose, a mechanical test of the monofilament yarns was carried out in a temperature chamber at increasing temperatures (180°C, 210°C, 240°C) in accordance with DIN EN ISO 2062.

TENSILE TEST ON COMPOSITE MATERIALS

As part of the present study, a tensile test was carried out on a composite material consisting of a GF/PP biaxial fabric and electrically conductive monofilament yarns (PEEK-MWCNT). The electrically conductive monofilament yarns were inserted into the GF/PP biaxial fabric in the warp direction and the tensile test was also carried out in the warp direction. The test was carried out in accordance with the DIN EN ISO 527-4 standard using a ZWICK/ROELL universal testing machine type Z100/MK 100 kN (Ulm, Germany). The measurement resulted in a clamping length of 150.00 mm with a preload setting of 15kN. A constant test speed of 2 mm/min was selected for the composite tensile test.

Textile Science & Research Journal
ISSN: 3059-846X Volume – 1, Issue – 1, 2025
DOI: https://doi.org/10.63456/tsrj-1-1-31

DETERMINATION OF THE ELECTRICAL RESISTANCE

The electrical resistance values of the MWCNT-containing PEEK filament yarns were determined in accordance with DIN 54345-5. The filament yarns were contacted on both sides using crimp connections in combination with conductive epoxy adhesive. The length-related resistance was measured using four-wire measurement technology (KEITHLEY DAQ 6510/7700, Solon, Ohio, US).

Since the melt-spun, MWCNT-containing PEEK filament yarns are used as temperature-resistant elongation sensor yarns in thermoplastic composites, the length-related electrical resistance was carried out with a simultaneous filament yarn tensile test. The test was carried out in accordance with the ISO 3341 standard on a Zwicki Z2.5 "Zwicki Jr." (Ulm, Germany) with a maximum force capacity of 2.5 kN and a crosshead with a torque of 10 Nm. Steel flat jaws with a surface area of 50 mm × 60 mm were used as the clamping device. To ensure a defined initial state, a preload of 10 N was applied before the start of the measurement. The Young's modulus was determined at a constant traverse speed of 10 mm/min. The subsequent tensile test until breakage was also carried out at a constant test speed of 10 mm/min. A clamping length of 250 mm was used for the filament yarn tensile test and the measuring length between two measuring electrodes was 160 mm for the length-related electrical resistance measurement. The electrical resistance measurement was carried out in accordance with DIN 54 345 T5 using a KEITHLEY DAQ 6510/7700 four-wire meter (Solon, Ohio, USA).

RESULTS AND DISCUSSIONS

3.1 DETERMINATION OF PHASE TRANSITIONS USING DIFFERENTIAL SCANNING CALORIMETRY (DSC)

The influence of MWCNT fillers on the thermal transitions of semi-crystalline PEEK was investigated using DSC by tracking the change in heat flow, which reflects the changes in the configurational degrees of freedom of the polymer during heating or cooling. Based on the DSC results, the semi-crystalline PEEK undergoes several thermal transitions called glass transition temperature (T_g), melting temperature (T_m) and crystallization temperature (T_c). In our DSC study (Figure 3), an T_g of 147.17°C was determined for pure PEEK, while the T_g for 7 wt.% MWCNT-reinforced PEEK was 150.91°C (Table 3). The present study showed a distinct increase in the T_g of PEEK with 7 wt.% MWCNT by 3 ± 1°C compared to pure PEEK. The DSC investigations exhibit that pure PEEK 151G has a high crystallinity. In a highly crystalline polymer, the proportion of amorphous areas is low. Since the glass transition occurs exclusively in the amorphous phase, the change in heat capacity associated with the T_g is very small. The T_g in the DSC diagram of pure PEEK is difficult or impossible to see (Figure 3). When MWCNTs are added, the crystallization behavior of pure PEEK changes. The crystallization temperature (T_{hc}) increases significantly with the addition of MWCNT, rising from 308.07°C for pure PEEK to approximately 318.08°C at 7 wt.% MWCNT, clearly demonstrating the pronounced heterogeneous nucleation effect of the MWCNTs (Table 3). The MWCNTs act as physical obstacles during the crystallization process and reduce the degree of order of the polymer chains. As a result, the overall crystallinity decreases and the proportion of the amorphous phase increases. With a higher amorphous content, the T_g becomes more clearly recognizable in the DSC, as the associated heat capacity change is now distinctly greater. In addition, interactions between the MWCNTs and the PEEK chains (e.g. via VAN DER WAALS forces or π-π interactions) can influence the mobility of the polymer chains and thus make the thermal transitions appear sharper or shifted. Overall, these effects lead to a clearer display of the T_g in the DSC diagram for PEEK-MWCNT blends. The values of Crystallization enthalpy (H_{hc}) and melting enthalpy (H_m) initially reach a maximum at low MWCNT contents and then decrease moderately. At higher MWCNT concentrations above 5 wt.%, the crystallinity becomes increasingly restricted, likely due to reduced mobility of the PEEK chains, possible MWCNT agglomeration, and the resulting blockage of the crystallization front.

Textile Science & Research Journal
ISSN:3059-846X Volume – 1, Issue – 1, 2025
DOI: https://doi.org/10.63456/tsrj-1-1-31

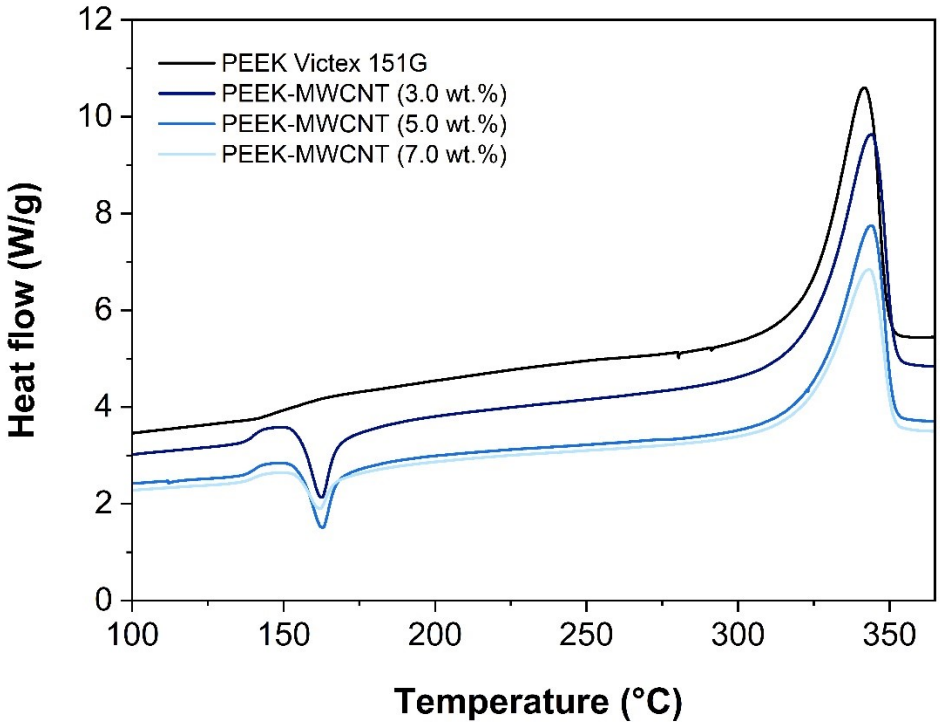

Figure 3. T_g and T_m of PEEK-MWCNT samples compared to pure PEEK after the first heating cycle.

In addition, investigations were carried out to evaluate the chain structure in the presence of MWCNTs. The focus was on the rigid and mobile amorphous fractions of the polymer chains. In the present study, the mobile amorphous fractions (X_{MAF}) and the rigid amorphous fractions (X_{RAF}) were calculated using the value of 0.27 J/g°C as $\Delta C_{\alpha p}$ according to the ADVANCED THERMAL ANALYSIS SYSTEM DATABASE [27,28] for PEEK. The $X_{(MAF)}$ value for pure PEEK is 61.33%, while the X_{RAF} value is 8.06% (Table 3). A decrease in the X_{MAF} value from 49.24% (1 wt.% MWCNT) to 37.18% (7 wt.% MWCNT) was observed with increasing MWCNT content in the PEEK. This means that the PEEK chain mobility is thereby restricted or that the proportion of the mobile amorphous phase of the polymer chains decreases. The X_{RAF} value for pure PEEK is 8.06%, while the value for MWCNT-PEEK blends is between 16.68% (1 wt.%). X_{RAF} showed a distinct increasing trend with respect to the amount of MWCNTs, and the highest X_{RAF} of 37.55% was obtained from 7 wt.% PEEK-MWCNT blends. The present study revealed that the embedding of MWCNTs in amorphous regions increased. It was found that the mobility of the polymer chains is restricted as a result. The observed effect is most likely the result of the wrapping of polymer chains by MWCNTs, coupled with synergistic binding between MWCNTs and the PEEK matrix, leading to an optimized interfacial region. The analysis of the X_{RAF} results (Table 3) shows a distinct correlation between the MWCNT content and the dispersion in the PEEK polymer matrix on the one hand and the crystallization behavior as well as the chain morphology on the other hand. The observed increase in the X_{RAF} with increasing MWCNT content indicates an increasing immobilization of PEEK chains in the vicinity of the MWCNT surfaces. The determined maximum X_{RAF} of 25.18% at 2% MWCNT suggests optimal dispersion and distinct polymer-filler interactions in this region. At higher concentrations, the effect decreases. This may be due to MWCNT agglomeration and reduced matrix-filler coupling.

Furthermore, the crystalline fraction (X_{CF}) for semi-crystalline PEEK polymers was taken into account. To gain a more comprehensive understanding, the crystalline fraction (X_{CF}) of pure PEEK and with MWCNT blends was calculated. The enthalpy of fusion (ΔH_f) of fully crystalline PEEK was taken from the literature at 130 J/g. [29, 27] The highest crystallinity was found to be 34.08% at 1 wt.% CNT in PEEK, while pure PEEK had 30.61% (Table 3). A decrease in crystallinity (25.27%) was observed with increasing MWCNT content (7 wt.%) in PEEK (Table 3). Similarly, studies by GOHN *et al.* [28] on PEEK composites reinforced with different amounts of CNTs showed a decrease in crystallization at higher MWCNT contents. These DSC results indicate that low filler concentrations facilitate nucleation and promote crystallization, while too high a filler content could hinder the crystallization process due to possible agglomeration and disruption of the polymer matrix.

Textile Science & Research Journal
ISSN: 3059-846X Volume – 1, Issue – 1, 2025
DOI: https://doi.org/10.63456/tsrj-1-1-31

Table 3. DSC results of pure PEEK and PEEK-MWCNT containing samples with the crystalline fraction (X_{CF}), the mobile amorphous fraction (X_{MAF}) and the rigid amorphous fraction (X_{RAF})

Samples	T_g (°C)	T_m (°C)	H_m (J/g)	T_{hc} (°C)	H_{hs} (J/g)	ΔCp (J/g°C)	X_{CF} (%)	X_{MAF} (%)	X_{RAF} (%)
PEEK151G/0/0	147.17	322.90	39.79	308.07	47.81	0.1656	30.61	61.33	8.06
PEEK/MWCNT (1.0 wt.%)	156.83	325.80	44.75	317.88	51.70	0.1343	34.08	49.24	16.68
PEEK/MWCNT (2.0 wt.%)	155.07	326.03	41.18	319.16	50.40	0.1206	31.04	43.77	25.18
PEEK/MWCNT (3.5 wt.%)	154.23	325.47	40.50	318.80	47.10	0.1046	30.06	37.38	32.55
PEEK/MWCNT (5.0 wt.%)	152.13	323.74	41.61	319.18	47.41	0.1086	30.41	38.21	31.38
PEEK/MWCNT (6.0 wt.%)	151.80	323.09	40.17	317.72	46.09	0.1242	28.74	42.78	28.48
PEEK/MWCNT (7.0 wt.%)	150.91	323.72	34.95	318.08	42.26	0.1068	25.27	37.18	37.55

Other publications have reported no drastic change in the melting temperature (T_m). [30, 29] The performed DSC measurement confirms this (Table 4 and Figure 4). The T_m values of the endothermic reaction in the DSC curve of pure PEEK were approx. 341.54°C during the first heating and with 7 wt.% MWCNT in PEEK at approx. 340.72°C also during the first heating cycle (Table 4). A marginal reduction in Tm with increasing MWCNT content in the PEEK samples was observed during both the initial and secondary heating phases (Table 4). The observation that the described behavior is similar in both cases (1st heating cycle and 2nd heating cycle) allows to presume that the MWCNTs remain permanently active as nucleating agents and systematically influence the crystallization behavior.

Compared to pure PEEK, the Tm increased by approx. 4°C with a MWCNT content of 1 wt.% in the PEEKMWCNT samples (Figure 4, left). With a further increase in the MWCNT content from 1 wt.% to 7 wt.%, the Tm fell from 345.38°C to 340.72°C. A slight decrease in Tm therefore implies the formation of larger but increased MWCNTs, as the MWCNTs act as multiple crystallization nuclei in this process. The decrease in Tm when increasing the MWCNT content in PEEK was confirmed by Gohn *et al*. [28] and Shang et al. [31]

Table 4. DSC results of pure PEEK and samples containing PEEK-MWCNT

Samples	1.Heating cycle		Cooling		2.Heating Cycle			Process Window
	T_m (°C)	X_c (%)	T_c (°C)	X_c (%)	T_m (°C)	X_c (%)	T_m-T_c (°C)	T_m-X_c (°C)
PEEK151G/0/0	341.54	36.3	303.77	42.31	343.26	40.18	37.77	14.83
PEEK/MWCNT (1.0 wt.%)	345.38	24.5	313.21	39.37	345	39.12	32.17	7.92
PEEK/MWCNT (2.0 wt.%)	343.7	22.89	313.34	37.99	345.5	38.13	30.36	6.87
PEEK/MWCNT (3.5 wt.%)	342.97	22.91	312.11	34.96	344.92	35.79	30.86	6.67
PEEK/MWCNT (5.0 wt.%)	343.08	22.57	312.19	34.65	345.15	33.97	30.89	4.56
PEEK/MWCNT (6.0 wt.%)	341.65	22.61	310.38	30.56	343.76	31.89	31.27	5.64
PEEK/MWCNT (7.0 wt.%)	340.72	21.98	309.99	32.97	342.98	34.01	30.73	5.37

Textile Science & Research Journal
ISSN:3059-846X Volume – 1, Issue – 1, 2025
DOI: https://doi.org/10.63456/tsrj-1-1-31

MWCNTs can act as heterogeneous nucleating agents in a PEEK polymer matrix. This can lead to increased crystallinity or accelerated crystallization. Crystallization, defined as an exothermic crystallization process observed between T_g and T_m temperatures, was not present in PEEK due to the lack of mobile polymer chains to form a regular one. The T_c and crystallinity decrease with increasing amount of MWCNTs (Figure 4, right). This shows that the Tc increased compared to pure PEEK at 10°C with 1 wt.% MWCNTs and at 6°C with 7 wt.% MWCNTs. T At low MWCNT concentrations (1 wt.%), the MWCNTs still have a supporting effect by providing crystallization nuclei. With increasing MWCNT content (7 wt.%), the agglomerations of the MWCNTs manifest themselves. It was found that the agglomeration of the particles leads to a reduction in the effective surface area and nucleation. The MWCNTs hinder the mobility of the PEEK chains, making it more difficult for the chains to align and crystallize.

As a result, fewer and more incomplete crystallites are formed. This results in reduced crystallinity and a lower T_c. This leads to a delay in crystallization and reduced crystallinity. This shift could be related to the additional heterogeneous nucleation sites initiated by MWCNTs. In previous studies, the addition of MWCNTs to a PEEK resulted in increased crystallinity, and the reason for these results was attributed to the presence of MWCNTs initiating nucleation and forcing an ordered shape. As previously stated, the increase in T_{hc} manifested itself in relation to the amount of MWCNTs as an indicator of heterogeneous nucleation sites, as documented in other MWCNT-PEEK studies.

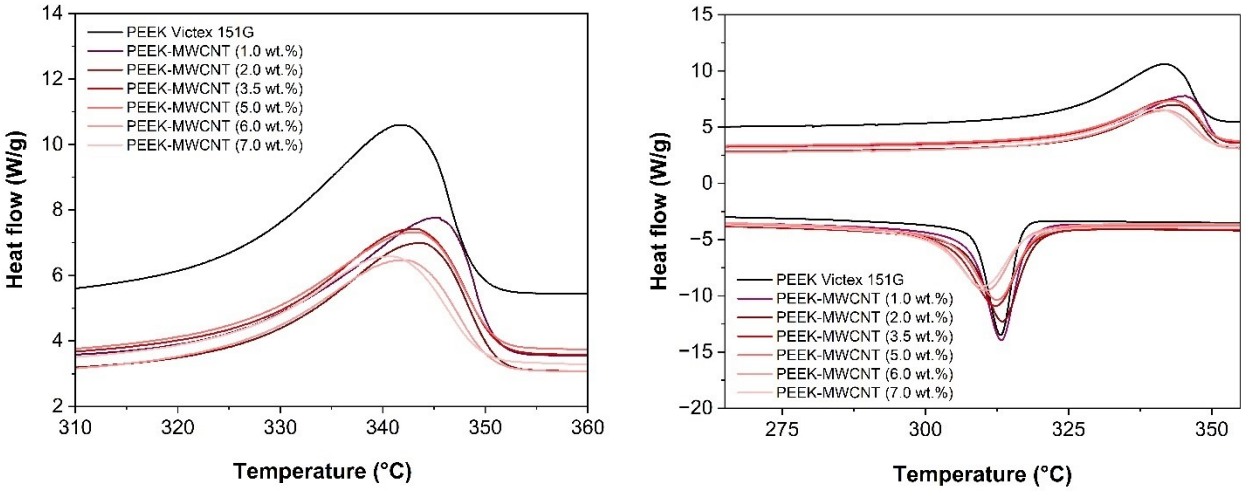

Figure 4. DSC thermograms of pure PEEK and PEEK-MWCNT samples compounded with the TSE ZSE 18 MAXX

40D, with focus on the melting areas (left) and with focus on melting range and crystallization (right) after first heating cycle

3.2 STABILITY AND DECOMPOSITION BEHAVIOR OF PEEK WITH AND WITHOUT MWCNTS

The mass change of PEEK as a function of temperature was determined by thermogravimetric analysis (TGA). The mass degradation rates and decomposition temperatures were recorded under oxidative (air) and inert (nitrogen) atmospheres. In both nitrogen and oxygen atmospheres, incipient decomposition of PEEK with and without MWCNTs was observed at around 565°C (Figure 5 and Figure 6). In an oxidative atmosphere, both the PEEK and the PEEK containing MWCNTs showed a two-stage decomposition, with the second stage being similar in nature to the first (Table 5, Figure 5 a and b). The maxima of the peaks of first derivative of TGA mass loss curves, which characterize the largest material conversions, were around 579°C and 692°C for PEEK without MWCNT in an oxidative atmosphere (Figure 5 c and d). The mass losses determined for PEEK amounted to 99.22 mass % in the temperature range of

500.07−699.66°C and 0.64 mass % in the range of 699.66−778.22°C (Table 5). In contrast, for PEEK with 1 wt.% MWCNT content, a lower mass loss of 47.68% was observed at a decomposition temperature between 499.72−788.21°C in the first degradation stage and 52.23 mass % at 788.21−981.43°C in the second degradation stage. It was found that as the MWCNT content in the PEEK increased, the mass loss decreased and the decomposition temperature decreased. At a concentration of 6wt.% MWCNT in PEEK, a low mass loss of 41.73 wt.% was observed at a decomposition temperature between 499.72−790.44°C in the first degradation stage and a high mass loss of 57.58 wt.% at 790.44–981.50°C in the second degradation stage

Textile Science & Research Journal
ISSN: 3059-846X Volume – 1, Issue – 1, 2025
DOI: https://doi.org/10.63456/tsrj-1-1-31

(Table 5). In summary, MWCNTs can be classified as extremely stable and thermally resistant materials and their decomposition can only be expected at distinctly higher temperatures above 1000°C. The decomposition temperature of the PEEK-MWCNT mixture was raised by 90°C by the introduction of MWCNTs. This results in a distinct improvement in the thermal stability of the PEEK-MWCNT mixtures. Furthermore, a slowing down of the decomposition rate of PEEK by MWCNT was observed. In addition, an improvement in heat transfer within the material was observed, which in turn led to a lower mass loss in the oxidative atmosphere (Table 5). Na *et al.*[24] and Silva *et al.* [25] confirm that MWCNTs have a high intrinsic thermal stability and that MWCNT networks inhibit the thermal movement behavior of the PEEK chains. This postpones the decomposition.

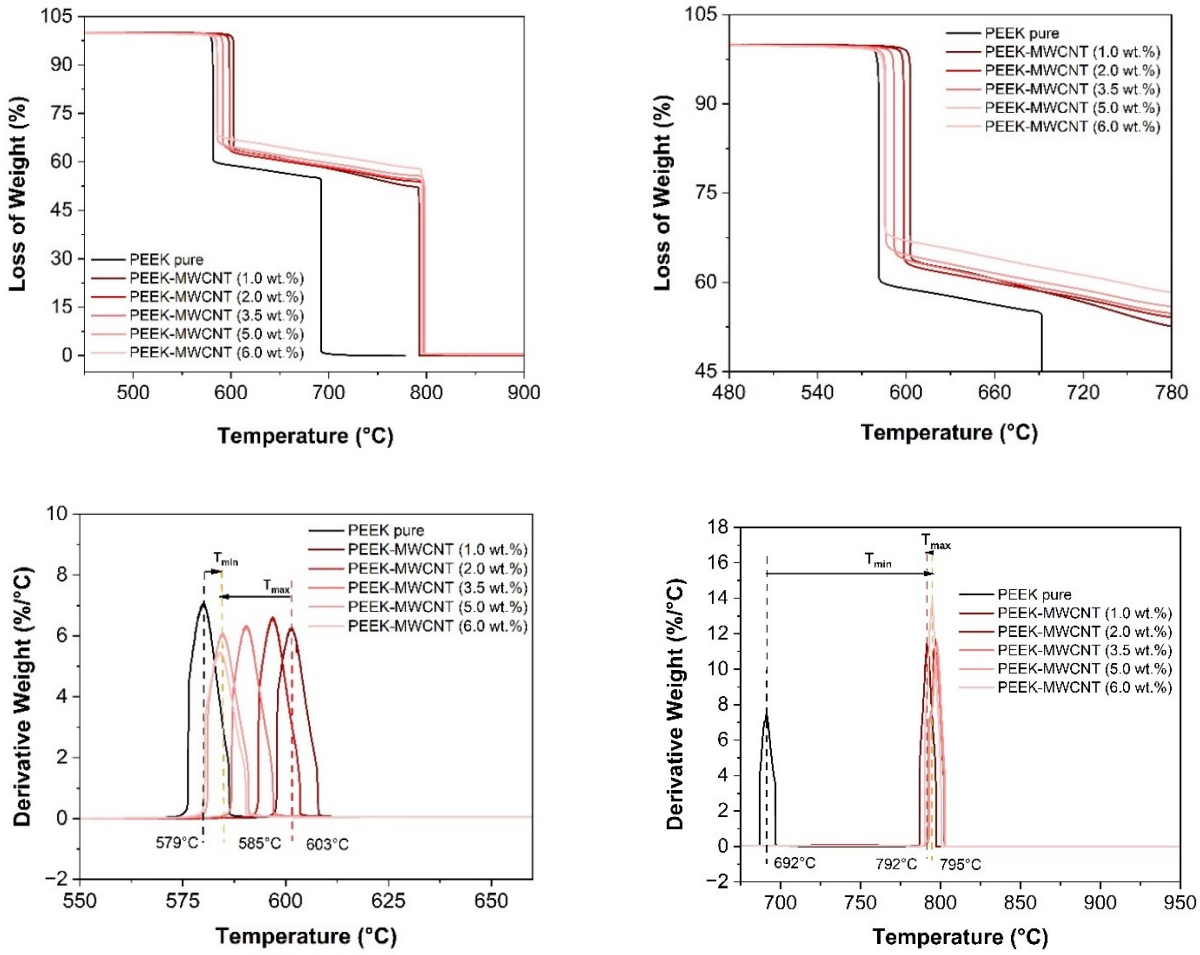

Figure 5. TGA curves of pure PEEK and their derivatives of MWCNT-reinforced PEEK materials in an air atmosphere at temperatures ranging from 450°C to 900°C (a), 480°C to 780°C (b), 550°C to 650°C (c) and 650°C to 950°C (d), compounded with a ZSE 18 MAXX 40D TSE.

In an inert atmosphere, however, only one-stage decomposition was observed (Figure 4a and 4b). The mass loss of PEEK, both with and without MWCNTs, was higher in the oxidative atmosphere and lower in the inert atmosphere (Table 5; Figure 6a and 6b). The decomposition temperature for pure PEEK was found to be 596°C in an inert atmosphere (Table 5; Figure 6). The highest decomposition temperature (608°C) was found for PEEK samples containing 1 wt.% MWCNT. The increasing proportion of MWCNTs in PEEK led to the opposite result, the decomposition temperature decreased from 593°C to 595°C and up to 589°C with 1 wt.%, 5 wt.% and 7 wt.% MWCNTs in PEEK. This behavior shows that the MWCNTs lowered the thermal energy in the pure PEEK due to the higher thermal conductivity of the decomposition temperature. Similarly, in an inert atmosphere, the degradation of PEEK without and with MWCNTs in a single step undergoes dehydration, decarboxylation and finally decarbonylation processes leading to water, carbon monoxide, carbon dioxide and phenols.

Textile Science & Research Journal
ISSN: 3059-846X Volume – 1, Issue – 1, 2025
DOI: https://doi.org/10.63456/tsrj-1-1-31

Table 5. Results of TGA of pure PEEK and their derivatives of MWCNT-reinforced PEEK materials in an air atmosphere.

Samples	1. Mass reduction		2. Mass reduction	
	T (°C)	Mass (%)	T (°C)	Mass (%)
PEEK pure	500.07 - 699.66	99.22	699.66 - 778.22	0.64
PEEK-MWCNT (1.0 wt.%)	499.72 - 788.21	47.68	788.21- 981.43	52.23
PEEK-MWCNT (2.0 wt.%)	499.72 - 791.19	46	791.19 - 981.53	53.58
PEEK-MWCNT (3.5 wt.%)	499.72 - 790.44	45.25	790,44 - 981.36	54.22
PEEK-MWCNT (5.0 wt.%)	499.72 - 791.19	44.07	791.19 - 981.53	55.26
PEEK-MWCNT (6.0 wt.%)	499.72 - 790.44	41.73	790.44 - 981.50	57.58

The decomposition temperature of PEEK without MWCNT (at 579°C) in air was higher than that of PEEK with MWCNT (6wt.%) at 585°C. Under nitrogen, the decomposition temperature of PEEK with the 6 wt.% MWCNT content was found to be 571°C, which is lower than PEEK without MWCNT (596°C). The associated mass loss was approximately 41.56% for PEEK and 36.16% for PEEK with 6 wt.% MWCNT (Figure 6; Table 5). The mass loss of PEEK-MWCNT in air in the first stage (99.22%) is therefore higher than in nitrogen (41.56%) (Table 4 and Table 5). The rapid weight loss below about 600°C is mainly due to the decomposition of phenols from PEEK at about 50 wt.%. $Tmax$ was found at 608°C for 1 wt.% MWCNT-containing PEEK and with MWCNT reinforcement, however, it decreased to about 571°C (Table 5; Figure 6). It was found that PEEK with MWCNT can be processed in both inert and oxidizing atmospheres, taking into account the mass loss.

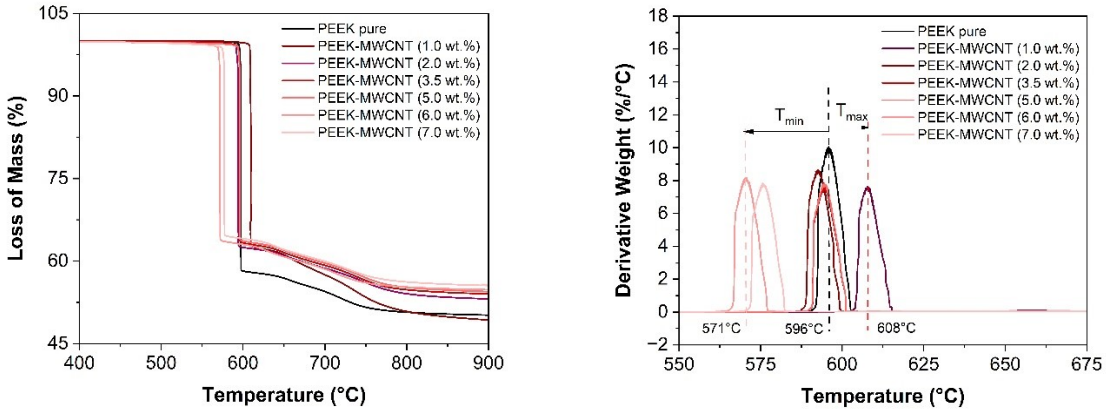

Figure 6. TGA curves of pure PEEK and their derivatives of MWCNT-reinforced PEEK materials in a nitrogen atmosphere at temperatures ranging from 400°C to 900°C (left) and 550°C to 675°C (right) compounding using a TSE ZSE 18 MAXX 40D.

The normal melt spinning temperature for PEEK without MWCNT takes place between 380°C and 400°C. Therefore, the thermal analysis confirms the compatibility and stability of the high performance, high viscosity PEEK without and with MWCNT. PEEK is a polymer consisting of repeated -C_6H_4-O-C_6H_4-C=O units, each containing an aromatic benzene ring (C_6H_4), an ether bridge (-O-) and a ketone group (-C=O-). This structure ensures that the PEEK polymer is highly rigid and stable, making it particularly resistant to high temperatures. Due to the aromatic stability of the benzene ring (C_6H_4), which is responsible for both thermal stability and the high strength of the polymer. The weakest bond in the bridging aromatic rings tends to initiate random cleavage, resulting in a remarkable stability of over 565 ° C (Figure 5 and Figure 6; Table 4 and Table 5).

The normal melt spinning temperature for PEEK without MWCNT takes place between 380°C and 400°C. Therefore, the thermal analysis confirms the compatibility and stability of the high performance, high viscosity PEEK without and with MWCNT. PEEK is a polymer consisting of repeated -C_6H_4-O-C_6H_4-C=O units, each containing an aromatic benzene ring (C_6H_4), an ether bridge (-O-) and a ketone group (-C=O-). This structure ensures that the PEEK polymer is highly rigid and stable, making it particularly resistant to high temperatures. Due to the aromatic stability of the benzene ring (C_6H_4), which is responsible for both thermal stability and the high strength of the polymer. The weakest bond in the bridging aromatic rings tends to initiate random cleavage, resulting in a remarkable stability of over 565 ° C (Figure 5 and Figure 6).

Textile Science & Research Journal
ISSN: 3059-846X Volume – 1, Issue – 1, 2025
DOI: https://doi.org/10.63456/tsrj-1-1-31

COMPOSITE MORPHOLOGY

The morphology and dispersion of MWCNT agglomerates were evaluated by scanning electron microscopy (SEM) on cross-sections of extruded PEEK/MWCNT filament yarns containing 1 to 7 wt.% MWCNT, as shown in Figure 7. The SEM analysis of the filament cross-sections (Figure 7) reveals a clear dependence of the microstructure on the MWCNT concentration. At low filler contents (1.0–3.5 wt.%), the samples exhibit a homogeneous and uniform distribution of nanotubes within the PEEK matrix (Figure 7b–d). In this concentration range, almost no large agglomerates are observed, indicating efficient dispersion and good wetting of the MWCNTs by the PEEK melt during the extrusion process.

With increasing MWCNT content (≥ 5 wt.%), larger agglomerates and irregularly distributed clusters become more pronounced (Figure 7e–g). These agglomerates form as a result of the higher particle density and the increased van der Waals attraction forces between neighboring nanotubes, which hinder their separation and uniform distribution during melt processing. At filler loadings between 5 and 7 wt.%, a clear saturation of the dispersion capacity of the PEEK matrix is observed, leading to locally concentrated MWCNT aggregates.

This behavior is consistent with the observations of Silva *et al.*, [25] who reported homogeneous dispersion in PEEK/MWCNT composites up to approximately 3 wt.% and a progressive agglomeration at higher concentrations. Silva *et al.* [25] also noted that the presence of larger agglomerates negatively affects the melt-spinnability of the composites, as they can induce local stress concentrations and filament breakage during spinning.

Overall, the SEM results suggest that an optimal MWCNT content for the PEEK/MWCNT system lies between 1 wt.% and 3.5 wt.%, where uniform dispersion and a homogeneous microstructure are achieved. Above this range, significant agglomeration occurs, which may adversely influence the mechanical and electrical properties as well as the spinnability and processability of the composite material.

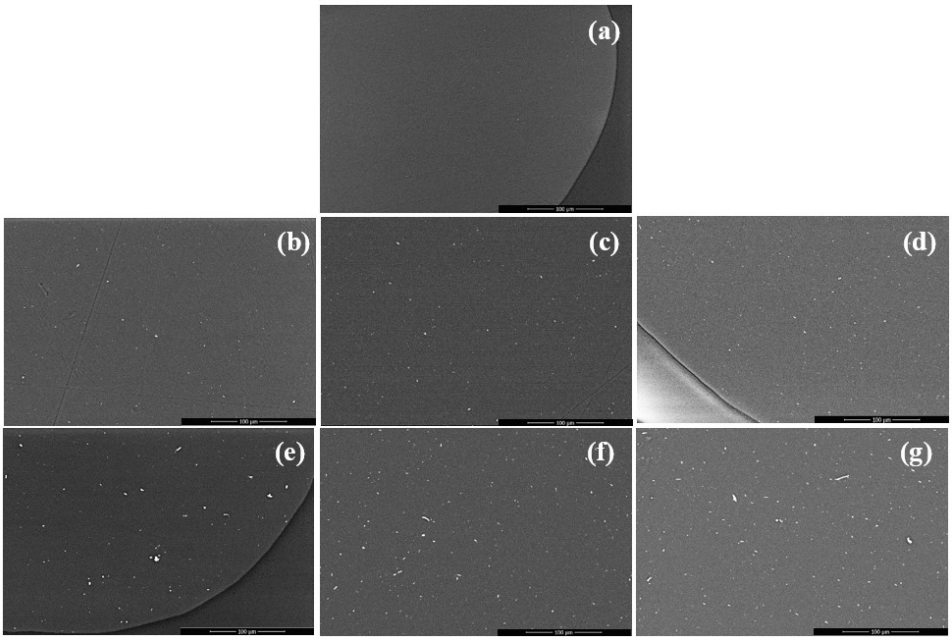

Figure 7. SEM micrographs (100 µm) of the cross-sections of (a) pure PEEK and PEEK containing increasing MWCNT concentrations: (b) 1.0 wt.%, (c) 2.0 wt.%, (d) 3.5 wt.%, (e) 5.0 wt.%, (f) 6.0 wt.%, and (g) 7.0wt.%.

MECHANICAL PROPERTIES

The experimental results show that with increasing MWCNT content, both the tensile strength and the Young's modulus of the monofilament yarns increased significantly (Table 6). This mechanical strengthening is due to the reinforcing effect of the well-dispersed MWCNTs within the PEEK matrix, which improves the load transfer within the material and increases the structural stiffness. At the same time, however, a decrease in elongation at break was observed with increasing MWCNT content (Table

Textile Science & Research Journal
ISSN:3059-846X Volume – 1, Issue – 1, 2025
DOI: https://doi.org/10.63456/tsrj-1-1-31

6). This behavior indicates an increased embrittlement of the material, which is characteristic for polymer-based nanocomposites with a high filler content. [33, 34] The reduced extensibility results from limited chain mobility caused by intense filler-matrix interactions and potential agglomeration structures within the polymer matrix. Although such interactions promote stiffness and strength, they significantly impair the ductility of the material. Gonçalves *et al*. [35] produced electrically conductive PEEK nanocomposite filaments incorporating carbon nanotubes and graphite nanoplatelets, and reported an improvement in Young's modulus and yield strength, while reducing the ductility of PEEK filaments.

Table 6. Influence of the increased MWCNT content (2.8 wt.%, 3.5 wt.%, 5.0 wt.%, 6.0 wt.% and 7.0 wt.%) on the mechanical properties of the PEEK-MWCNT monofilament yarns

Sample No.	MWCNT content in pure PEEK	Young's modulus (GPa)	Elongation at Break (%)	Tensile strength (MPa)
1	0.0 wt.%	1.64 ± 0.45	161.7 ± 35.3	51.62 ± 14.81
2	3.5 wt.%	1.9 ± 0.06	3.9 ± 1.7	88.63 ± 21.79
3	5.0 wt.%	2.8 ± 0.11	3.6 ± 1.6	96.47 ± 34.37
4	6.0 wt.%	5.5 ± 0.17	2.9 ± 1.2	116.14 ± 38.33
5	7.0 wt.%	6.0 ± 0.13	2.0 ± 1.3	102.78 ± 30.01

The mechanical properties of the investigated PEEK and PEEK-MWCNT filaments show a clear dependence on temperature, MWCNT content, and filament structure. For all samples, the Young's modulus decreases significantly with increasing temperature (Table 7). For example, the Young's modulus of PEEK multifilaments without MWCNT decreases from 8.46 GPa at 25 °C to 0.79 GPa at 200 °C. At the same time, the elongation at break increases, indicating enhanced polymer chain mobility and reduced stiffness at higher temperatures. The addition of MWCNTs affects filament stiffness and ductility differently. With increasing MWCNT content, elongation at break decreases. At low MWCNT content (0.5 wt.%) in core-sheath filaments, an extremely high elongation at break is observed (466.8 % at 25 °C), while the E-modulus (0.20 GPa) remains low, particularly at elevated temperatures (210 °C). At high MWCNT content (3.5 wt.%) in PEEK monofilaments, the Young's modulus increases to 6.55 GPa at room temperature, whereas elongation at break is reduced (54.4 %), indicating higher stiffness due to the nanofillers. With increasing temperature (240 °C), elongation at break rises from 54.4 % to 223.7 %, while the Young's modulus decreases from 6.55 GPa to 0.46 GPa (Table 7). Filament structure also strongly influences mechanical performance. Core-sheath filaments exhibit particularly high ductility at room temperature, whereas monofilaments with high MWCNT content are stiffer but less stretchable. Multifilaments without MWCNT show intermediate Young's modulus values and moderate elongation at break. Overall, the results highlight a pronounced interplay between temperature, MWCNT content, and filament structure on the mechanical properties of PEEK filaments. Increasing temperature softens the material while enhancing ductility due to increased polymer chain mobility. Low MWCNT contents significantly improve ductility, whereas high contents primarily increase stiffness. Filament structure further modulates these effects: core-sheath filaments are particularly suitable for applications requiring high elongation, while stiff monofilaments are advantageous in mechanically demanding structures.

Table 7. Influence of the MWCNT content on the mechanical properties of the different PEEK-MWCNT filament yarns

Sample No.	PEEK-Filament	T,°C	MWCNT content in pure PEEK	T_{tex}, tex	Young's modulus (GPa)	Elongation at Break (%)
1	PEEK-Multifilament	25	0.0 wt.%	32.57	8.46	75.4
2		180	0.0 wt.%	32.57	1.80	113.1
3		200	0.0 wt.%	32.57	0.79	157.1
4	Core-sheath filament yarns	25	0.5 wt.%	293.3	1.47	466.8
5		180	0.5 wt.%	293.3	0.13	152.4
6		210	0.5 wt.%	293.3	0.20	195.0
7	PEEKMWCNT-Monofilament	25	3.5 wt.%	2000	6.55	54.4
8		180	3.5 wt.%	2000	0.59	159.5
9		210	3.5 wt.%	2000	0.47	298.9
10		240	3.5 wt.%	2000	0.46	223.7

Textile Science & Research Journal
ISSN: 3059-846X Volume – 1, Issue – 1, 2025
DOI: https://doi.org/10.63456/tsrj-1-1-31

Another relevant parameter for the targeted adjustment of the mechanical properties of melt-spun filament yarns is the yarn take-off speed in the spinning process. In the present study, its influence on the mechanical properties of C-S filament yarns consisting of an electrically conductive PEEK-MWCNT core (0.5 wt.% MWCNT) and a PEEK sheath was systematically analyzed. A comparison of the filament yarns drawn off at 90 m/min and 100 m/min showed that the elongation at break increased significantly from 383% to 393% and the Young's modulus increased significantly from 0.93 GPa to 1.5 GPa as the draw-off speed increased (Figure 8, left). A further increase in the pull-off speed to 110 m/min led to a slight reduction in the elongation at break from 383% to 342%, with the Young's modulus remaining at the previously achieved level. At a pull-off speed of 120m/min, the elongation remained unchanged at 344%, while the Young's modulus increased again and reached a maximum value of 1.7 GPa. The increased draw-off speed therefore has a clear effect on the orientation of the polymer chains in the filament: Faster cooling and tensile stress in the solid state lead to an increased chain orientation in the spinning direction, which increases stiffness but simultaneously reduces extensibility. These typical structure-property correlations can be observed particularly in high-temperature processed thermoplastic filaments. The extruder parameters were kept constant during all tests. The speeds of the twinscrew extruder for the PEEK- MWCNT core and the single-screw extruder for the PEEK sheath were both 5 rpm. The observed effect can therefore be clearly attributed to the variation in draw-off speed.

In further investigations, the influence of the extruder speed of the PEEK sheath on the mechanical properties of melt-spun C-S filament yarns were analyzed (Figure 8, right). Here, the speed of the single-screw extruder for the PEEK sheath component was increased from 5 rpm to 10 rpm, while the speed of the twin-screw extruder for the PEEK/MWCNT core (0.5 wt.% MWCNT) was kept constant at 5 rpm. The filament yarns were then wound onto bobbins at varying draw-off speeds (100 m/min, 120 m/min and 140 m/min). A direct comparison of the filament yarns produced at the same draw-off speed (100 m/min) showed that the samples with a higher sheath extruder speed (10 rpm) had a significantly lower Young's modulus of 0.89 GPa, compared to 1.5 GPa at the lower speed (5 rpm), as shown in Figure 8 (left and right). This difference can be attributed to the change in rheology and layer structure during coextrusion: Increased speed of the PEEK sheath material can lead to non-uniform distribution, lower chain orientation or internal stresses that negatively affect the mechanical stiffness of the filament. With increasing draw-off speed (120 m/min and 140 m/min), an increase in both the Young's modulus and elongation at break was observed in the samples extruded at 10 rpm. The highest Young's modulus of 1.5 GPa was achieved at a draw-off speed of 140 m/min. This increase is directly related to the improved warp orientation along the spinning direction due to the higher mechanical elongation during yarn take-off. These results underline the complex interaction between extrusion parameters and spinning conditions in the production of functionalized C-S filament yarns. In particular, the sheath extruder speed has a significant effect on the microstructural formation and thus on the resulting mechanical properties.

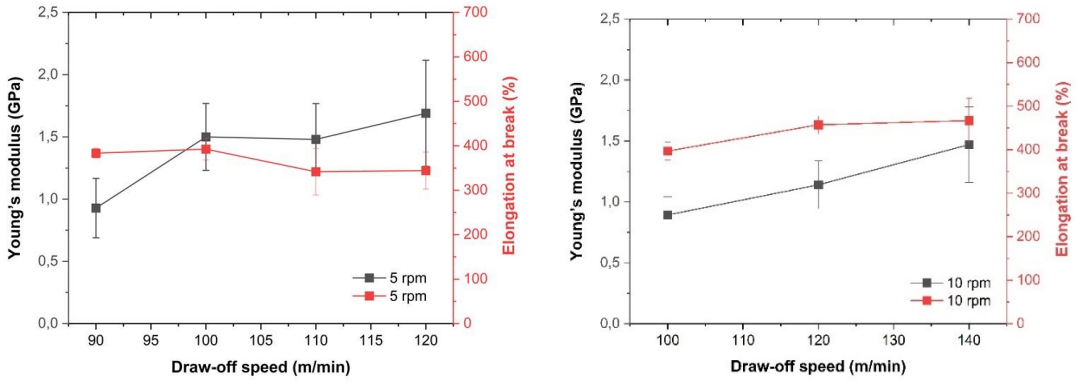

Figure 8. Influence of the draw-off speed (90 m/min, 100 m/min, 110 m/min, 120 m/min and 140 m/min) on the mechanical properties of C-S filament yarn (PEEK-MWCNT core and PEEK sheath), constant speed of the TSE for PEEK-MWCNT (5 rpm) and the speed of the SSE for PEEK ((left) 5 rpm and (right) 10 rpm).

To classify the PEEK-based filament yarns produced as part of this work, their mechanical properties were compared with commercially available, pure PEEK filament yarn. The latter, produced from commercially available PEEK without MWCNT content, exhibit typical mechanical characteristics: The Young's modulus is in the range of 3.6−4.1 GPa, the tensile strength is 90−100 MPa, and the elongation at break varies between 20% and 80% depending on the process control. [16, 19] For comparison, monofilament yarns made of pure VICTREX™ PEEK 151G, which was processed without MWCNT, were also melt-spun in our own test setup. These yarns achieved an elongation of 155%, a Young's modulus of 1.7 GPa and a tensile strength of 50MPa. Their mechanical properties and tensile strength are therefore between those of commercial filaments, but the elongation and Young's modulus are lower.

Textile Science & Research Journal
ISSN: 3059-846X Volume – 1, Issue – 1, 2025
DOI: https://doi.org/10.63456/tsrj-1-1-31

For strain sensors, the target value for elongation is typically less than 5%. The PEEK-MWCNT monofilament yarns produced using the melt spinning process with a filler content of 3.5 wt.% MWCNT achieve this target value, but exhibit significantly reduced mechanical properties compared to commercial pure PEEK filament yarns. The measured Young's modulus was on average 1.7 ± 0.2 GPa, the elongation at break was 4 ± 1%. These limitations of the mechanical properties can be attributed to the reduced chain mobility and possible agglomeration of the MWCNTs. These impair the microstructure of the composite material and thus negatively influence the elongation behavior.

The C-S filament yarns developed with an electrically conductive PEEK-MWCNT core (0.5 wt.%) and a pure PEEK sheath showed contrasting behavior. Despite a comparatively low Young's modulus of 1.3 ± 0.2 GPa, these yarns exhibited an exceptionally high elongation at break of 380 ± 20%. This combination of flexibility and functionalized conductivity opens up potential applications in flexible high-performance composites or smart textile structures.

It is noteworthy that increasing the draw-off speed during the spinning process led to a simultaneous increase in Young's modulus and elongation in both the pure PEEK yarns and the MWCNT-containing filament yarns. This observation points to complex interactions between melt flow, interphase adhesion and the orientation of the polymer chains during stretching - effects that can be used specifically in process optimization to modulate the mechanical property profile of the filaments.

TENSILE STRENGTH OF COMPOSITE

Table 8 presents the mechanical behavior of GF/PP composite sheets reinforced with integrated PEEK/MWCNT–PEEK core–sheath (C–S) filament yarns processed under different spinning conditions. The composites were produced using a constant screw speed of 5 rpm for the PEEK/MWCNT core (TSE) and screw speeds of 5 and 10 rpm for the PEEK sheath (SSE). The results were compared with a reference composite without integrated sensor yarns. The reference GF/PP composite (sample 1) exhibited a Young's modulus of 11.4 ± 1.45 GPa, a tensile strength of 288.99 ± 33.74 MPa, and an elongation at break of 2.8 ± 0.2%. The integration of C–S sensor yarns (samples 2–7) modified these properties depending on the pull-off speed and processing parameters. In general, the addition of the conductive PEEK/MWCNT–PEEK filament slightly reduced the stiffness at low processing speeds but improved tensile strength and, in some cases, ductility, indicating effective stress transfer between the sensor yarn and the GF/PP matrix.

At a constant SSE speed of 5 rpm, increasing the pull-off speed from 90 to 110 m/min resulted in a continuous improvement in mechanical performance of composite materials. The Young's modulus increased from 9.07 ± 0.69 GPa (90 m/min) to 13.1 ± 2.28 GPa (110 m/min), and the tensile strength rose from 301.97 ± 29.23 MPa to

338.4 ± 37.27 MPa. The elongation at break remained nearly constant (≈3%). This trend suggests that moderate increases in pull-off speed enhance the molecular orientation and interfacial bonding between core and sheath as well as between the sensor yarn and surrounding GF/PP matrix. The higher take-up rate likely promotes improved filament alignment and densification during composite consolidation, leading to more efficient load transfer and enhanced strength.

When the SSE screw speed was increased to 10 rpm (samples 5–7), a similar but less pronounced behavior was observed. At 110 m/min, the composite exhibited the highest tensile strength (324.6 ± 49.5 MPa) and modulus (13.3 ± 1.18 GPa), comparable to the best-performing sample from the 5 rpm series. However, further increasing the pull-off speed to 120–140 m/min caused a gradual decrease in modulus and strength (down to 10.7 ± 1.39 GPa and 308.5 ± 16.7 MPa, respectively). This indicates that excessively high take-up rates can induce microstructural defects such as voids, imperfect fiber wetting, or partial delamination of the sensor yarn within the composite. These defects reduce effective stress transfer and compromise mechanical stability, despite the initially favorable molecular orientation at intermediate speeds.

Overall, the results reveal a non-linear relationship between pull-off speed and the mechanical response of the GF/PP composites containing PEEK/MWCNT–PEEK sensor yarns. An optimal processing window appears around 110 m/min, where both modulus and tensile strength reach their maximum values for both SSE speeds. At this point, improved core–sheath cohesion and enhanced matrix impregnation likely compensate for the local stiffness mismatch introduced by the conductive core. Interestingly, even though the integration of the C–S filament introduces a second thermoplastic phase (PEEK within GF/PP), the overall mechanical performance remains comparable or superior to that of the reference composite. This indicates that the mechanical coupling between the sensor yarn and the composite matrix is efficient and that the PEEK-based filament can be embedded without weakening the composite structure.

The findings demonstrate that the mechanical integrity of the GF/PP composite is maintained, or even slightly improved, after

Textile Science & Research Journal
ISSN: 3059-846X Volume – 1, Issue – 1, 2025
DOI: https://doi.org/10.63456/tsrj-1-1-31

integrating the PEEK/MWCNT–PEEK sensor yarn. Optimal spinning and pull-off conditions (TSE 5 rpm, SSE 5–10 rpm, pull-off ≈110 m/min) yield the highest stiffness and tensile strength, reflecting efficient fiber orientation and matrix–sensor adhesion. At higher pull-off speeds (>120 m/min), minor decreases in strength and modulus indicate the onset of process-induced imperfections. Therefore, precise control of spinning speed and yarn integration parameters is crucial to ensure both reliable sensor functionality and mechanical performance of the composite system.

Table 8. Influence of the integrated PEEK/MWCNT-PEEK C-S filament yarns as sensor yarn on the mechanical properties of the GF/PP composite sheets, constant speed (5 rpm) of the TSE for PEEK-MWCNT and the speed 5 rpm and 10 rpm of the SSE for PEEK.

Sample no.	Core-sheath filament yarn	Speed (rpm)		Pull-off speed (m/min)	Young's modulus (GPa)	Tensile strength (MPa)	Elongation at break (%)
		TSE	SSE				
1	without	-	-	-	11.4 ± 1.45	288.99 ± 33.74	2.8 ± 0.2
2	Core (PEEK-MWCNT (0.5 wt.%) - Sheath (PEEK)			90	9.07 ± 0.69	301.97 ± 29.23	2.7 ± 0.5
3		5	5	100	9.76 ± 1.1	313.77 ± 8.53	3.1 ± 0.2
4				110	13.1 ± 2.28	338.4 ± 37.27	3.1 ±0.5
5				110	13.3 ± 1.18	324.58 ± 49.48	2.8 ± 0.4
6		5	10	120	11.9 ± 2.59	287.42 ± 20.3	2.6 ± 0.3
7				140	10.7 ± 1.39	308.46 ± 16.65	3.0 ± 0.1

CROSS-SECTIONAL AREA OF THE YARN FOR CALCULATING THE SPECIFIC ELECTRICAL RESISTANCE PEEK-MWCNT MONOFILAMENT YARN

For the precise determination of the specific electrical resistance of melt-spun filament yarns, the exact determination of the cross-sectional area is of crucial importance, as the electrical resistance depends significantly on the geometry and size of the material. The images taken by light microscopy showed that the monofilament yarns do not have the ideal round cross-section, but an oval shape (Figure 9). The measured cross-sectional dimensions were 3.5 ± 0.1 mm on the longer axis and 2.4 ± 0.1 mm on the shorter axis (Figure 9). The consideration of this oval geometry is essential in order to precisely determine the specific electrical resistance and thus to be able to make reliable statements about the conductivity of the PEEK-MWCNT monofilament yarns.

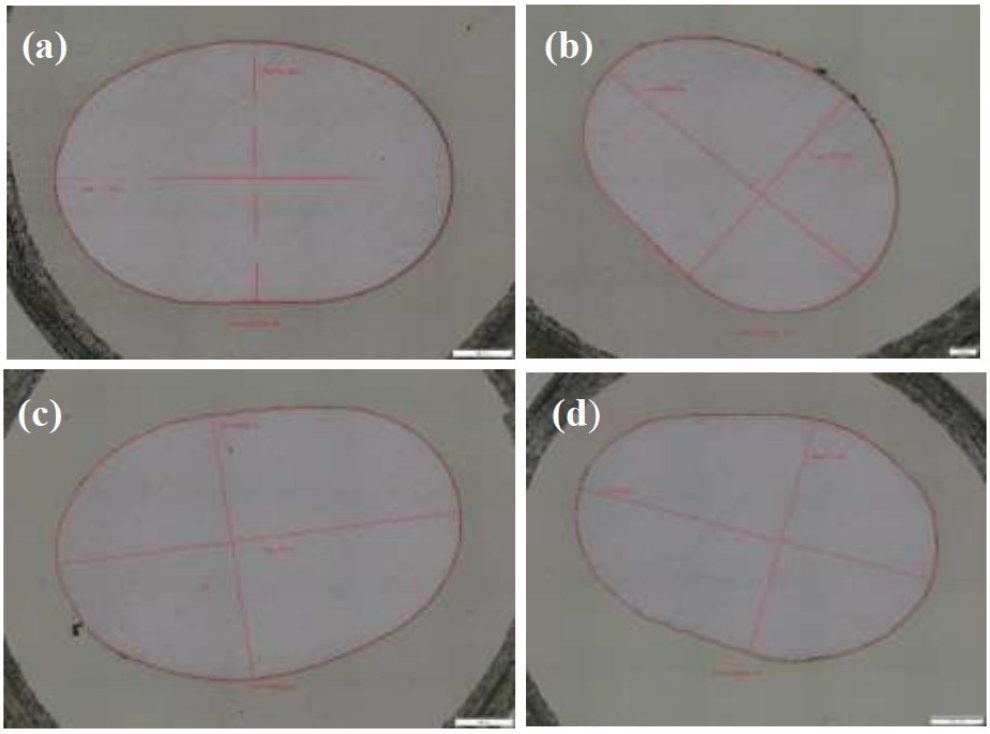

Figure 9. Cross-section of PEEK-MWCNT monofilament yarns composed and melt-spun using a ZSE 18 MAXX 40D TSE with increasing of MWCNT in the PEEK ((a) 3.5 wt.%, (b) 5.0 wt.%, (c) 6.0 wt.% and (d) 7.0 wt.%).

Textile Science & Research Journal
ISSN: 3059-846X Volume – 1, Issue – 1, 2025
DOI: https://doi.org/10.63456/tsrj-1-1-31

The determined cross-sectional area of the PEEK-MWCNT monofilament yarns was in the range of 1.66 mm² to 1.82 mm² (Table 9). The evaluation of the measurement results shows that the cross-sectional area of the produced PEEK-MWCNT monofilaments remains largely constant despite variations in MWCNT content. Overall, this indicates that the fiber formation process is stable and highly reproducible at the investigated MWCNT concentrations, without leading to significant changes in cross-sectional area. Larger filament diameters generally result in more homogeneous stress distribution and reduced surface defect sensitivity, which can lead to higher apparent tensile strength and modulus (Table 6). This finding suggests that microstructural factors such as MWCNT alignment, interfacial adhesion, and degree of agglomeration dominate over purely geometric effects. The small but consistent differences in area within each series thus act as secondary contributors that amplify or mitigate the primary microstructural effects induced by processing and composition.

Table 9. Determined mean value of the area of the melt-spun PEEK-MWCNT monofilament yarn

Samples No.	Compound	MWCNT (wt.%)	Area (mm^2)
1	PEEK-MWCNT using TSE ZSE 18 MAXX 40D	3.5	1.66 ± 0.12
2		5.0	1.83 ± 0.15
3		6.0	1.70 ± 0,09
4		7.0	1.77 ± 0.15

C-S FILAMENT YARN MADE OF PEEK-MWCNT (0.5 WT.%) AS CORE AND PEEK AS SHEATH

The thickness of the PEEK sheath layer, the diameter of the electrically conductive PEEK-MWCNT core (0.5 wt.%) and the exact position of the core within the sensor yarn are decisive parameters for avoiding short circuits in C-S structures. For the production of C-S filament yarns, the machine parameters - in particular the yarn draw-off speed (90-140 m/min) and the extruder speeds - have a decisive influence on the yarn morphology. The core, consisting of a conductive PEEK-MWCNT compound, was processed in a TSE, while the sheath, made of pure PEEK, was produced in a SSE.

In the first step, the speeds of the TSE and SSE were each set to a constant 5 rpm. Subsequently, only the yarn take-off speed was increased step by step from 90 m/min to 100 m/min up to 110 m/min. As the draw-off speed increased, the electrically conductive PEEK-MWCNT core showed increasing one-sidedness, while the insulating layer of pure PEEK did not completely enclose the core structure at individual points (Figure 10). It was not possible to achieve a centered core layer with a uniform cladding layer (Figure 10). In addition, the yarn cross-sectional thickness of the melt-spun PEEK-MWCNT/PEEK C-S filament yarn decreased with increasing draw-off speed.

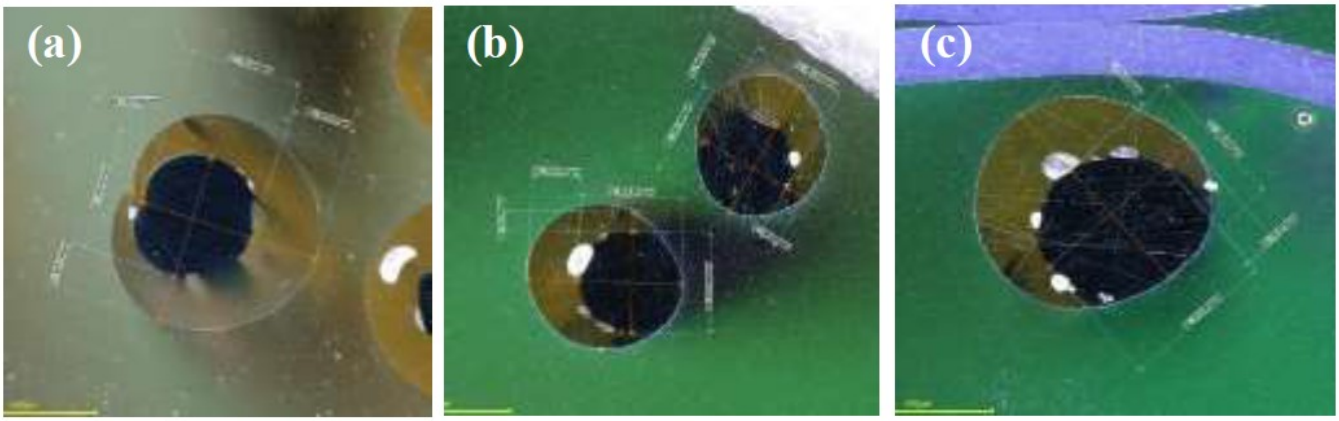

Figure 10. Influence of the draw-off speed of (a) 90 m/min, (b) 100 m/min and (c) 110 m/min on the cross-section of the C-S filament yarns, with a 5 rpm TSE speed for the PEEK-MWCNT core and with a 5 rpm SSE speed for the PEEK sheath.

The longitudinal view of the manufactured textile conductor structure clearly showed that the conductive core made of PEEK-MWCNT is not positioned centrally within the yarn (Figure 11). The surrounding PEEK sheath has a pronounced asymmetrical geometry, which led to a one-sided coating of the core.

Textile Science & Research Journal
ISSN: 3059-846X Volume – 1, Issue – 1, 2025
DOI: https://doi.org/10.63456/tsrj-1-1-31

Figure 11. Influence of the take-off speed of (a) 90 m/min, (b) 100 m/min and (c) 110 m/min on the longitudinal view of the C-S filament yarns. with a 5 rpm TSE speed for the PEEK-MWCNT core and with a 5 rpm SSE speed for the PEEK sheath.

In further tests, the speed of the SSE was increased from 5 rpm to 10 rpm, while the speed of the TSE for the PEEK-MWCNT core was kept constant at 5 rpm. Despite an increased yarn draw-off speed of 100 m/min to 140 m/min, no centric positioning of the PEEK-MWCNT core in the filament yarn could be observed (Figure 12).

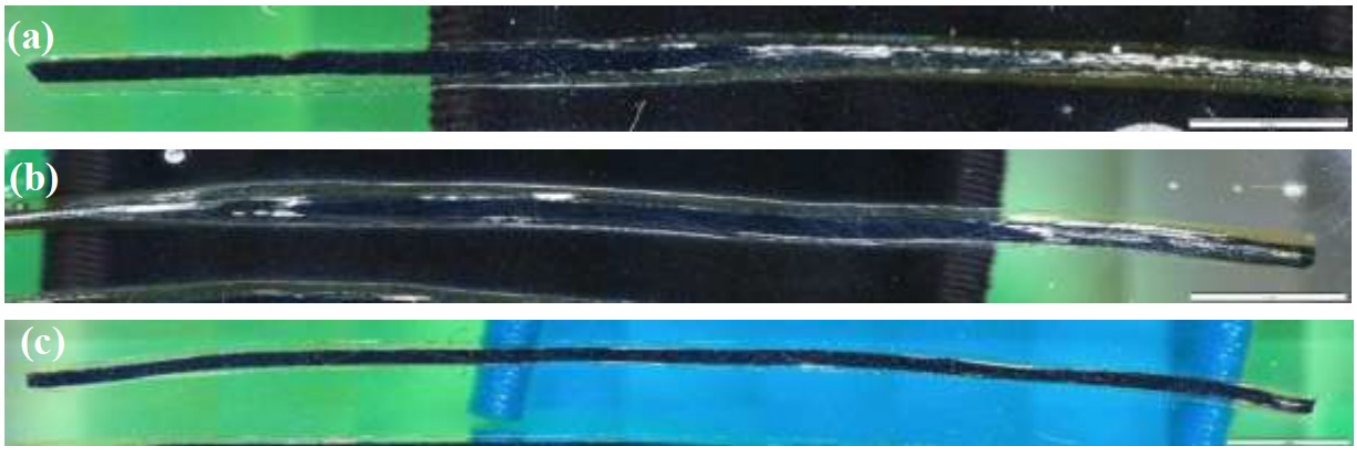

Figure 12. Influence of the draw-off speed of 100 m/min (a), 120 m/min (b) and 140 m/min (c) on the longitudinal view of the core-sheath filament yarns. with a 5 rpm twin-screw extruder speed for the PEEK/MWCNT core and with a 10 rpm single-screw extruder speed for the PEEK sheath.

Table 10 compares the diameter of the C-S filament yarns as a function of the yarn draw-off speed and the speeds of the SSE. It can be seen that the total diameter of the C-S filament yarns decreases with increasing draw-off speed.

Table 10. Diameter of the melt-spun C-S filament yarn made of PEEK-MWCNT/PEEK as a function of the increasing draw-off speed and speed of the SSE

Sample no.	Yarn	Speed (rpm)		Take-off speed (m/min)	Diameter (mm)
		TSE	SSE		
1	Core (PEEK-MWCNT (0.5 wt.%) - Sheath (PEEK)	5	5	90	0.64±0.01
2				100	0.57±0.02
3				110	0.54±0.03
4		5	10	110	0.73±0.02
5				120	0.65±0.03
6				140	0.57±0.21

Textile Science & Research Journal
ISSN: 3059-846X Volume – 1, Issue – 1, 2025
DOI: https://doi.org/10.63456/tsrj-1-1-31

The comparison of the core diameters and sheath thicknesses, based on cross-sectional images of all samples as a function of the yarn draw-off speed and the speeds of the TSE and SSE, is shown in Table 11. As the draw-off speed increased, not only did the total diameter of the C-S filament yarn decrease, but the diameter of the PEEKMWCNT core and the thickness of the PEEK sheath were also reduced (Table 11). At a yarn take-off speed of 110 m/min and constant speeds of 5 rpm for both the ESE (PEEK sheath) and the DSE (PEEK-MWCNT core), a core diameter of 264.73 ± 8.34 µm and a sheath thickness of 124.74 ± 7.01 µm at the thickest and 44.36 ± 10.2 µm at the thinnest point were measured (Table 11). With an unchanged yarn take-off speed of 110 m/min and a constant TSE speed of 5 rpm, but increased SSE speed from 5 rpm to 10 rpm, the core diameter increased to 391.13 ± 43.01 µm. The cladding thickness was 175.39 ± 34.32 µm at the thickest point and 33.04 ± 9.79 µm at the thinnest point (Table 11).

Table 11. Core diameter and sheath thickness of the melt-spun C-S filament yarn

Samples No.	Yarn	Speed (rpm)		Draw-off speed (m/min)	Core diameter (µm)	Sheath layer	
		TSE	SSE			Thick side (µm)	Thin side (µm)
1	Core (PEEK-MWCNT (0.5 wt.%) - Sheath (PEEK)	5	5	90	456.25±47.49	143.87±20.49	60.34±5.8
2				100	370.95±35.43	173.59±9.38	62.36±10.1
3				110	264.73±8.34	124.74±7.01	44.36±10.2
4		5	10	110	391.13±43.01	175.39±34.32	33.04±9.79
5				120	328.95±3.14	157.79±32.30	43.35±23.62
6				140	315.84±16.61	158.89±29.55	30.77±4.71

The observed decentration of the PEEK-MWCNT core and the one-sided formation of the PEEK cladding (Figure 10 and Figure 11) indicate a significant optimization potential in the manufacturing process of the coaxial corecladding structure. A symmetrical distribution of the sheath is desirable from both an electrical and mechanical perspective, as it ensures a homogeneous insulation effect and uniform mechanical load distribution. Targeted process adjustments should be investigated and implemented in the future to improve structural homogeneity.

CONTACTING

For the integration of melt-spun, electrically conductive monofilament yarns (PEEK-MWCNT) and melt-spun C-Sfilament yarns as sensor yarns in GF/PP composite panels, reliable electrical contacting of the sensor yarns is of central importance. The combination of crimp and epoxy adhesive connection (epoxy conductive paste) achieved the best contacting results, i.e. the lowest contact resistance and the most stable measurement results. The electrical resistance of the PEEK/MWCNT monofilament yarns produced using the melt spinning process was measured before and after contacting using a crimp connection and conductive epoxy adhesive. The results (Table 12) show that both the electrical contact resistance and the fluctuations in the measured values were significantly reduced by the combined use of crimping technology and conductive epoxy adhesive. This optimization of the contacting led to an overall improvement in the electrical conductivity of the connection (Table 12).

Table 12. Electrical resistance before and after contacting the PEEK-MWCNT monofilament yarn

Samples	Resistance before contacting (Ω)	Resistance after contacting (Ω)
MWCNT (3.5 wt.%)	19200 ± 5700	6120 ± 1800
MWCNT (5.0 wt.%)	5700 ± 2200	2340 ± 400
MWCNT (6.0 wt.%)	3800 ± 900	1780 ± 100
MWCNT (7.0 wt.%)	3400 ± 1300	1560 ± 100

Textile Science & Research Journal
ISSN: 3059-846X Volume – 1, Issue – 1, 2025
DOI: https://doi.org/10.63456/tsrj-1-1-31

RESISTANCE

With regard to the development of temperature-resistant and stretchable PEEK-MWCNT sensor yarns, the elongation of PEEK-MWCNT filament yarn in relation to the absolute electrical resistance was investigated. Electrically conductive PEEK-MWCNT monofilament yarns with different MWCNT contents (3.5 wt.%, 5.0 wt.%, 6.0 wt.% and 7.0 wt.%) were used, which were melt-spun from appropriately compounded pellets. The results in Figure 13 (a and b) show that the absolute resistance at lower MWCNT contents (3.5 wt.% and 5.0 wt.%) of around 7000 Ω and 4000 Ω respectively is significantly higher and more affected by noise than at higher MWCNT contents of 6.0 wt.% and 7.0 wt.%. At the same time, the PEEK-MWCNT monofilament yarn with 3.5 wt.% MWCNT has a comparatively high elongation of 4.2%, while the elongation decreases with increasing MWCNT content (Figure 13a). At 7.0 wt.% MWCNT, the lowest resistance of approx. 1500 Ω and the lowest elongation of 1.5% and minimized noise in the resistance were measured (Figure 13d). These results illustrate the typical trade-off between electrical conductivity and mechanical ductility in polymer-based nanocomposites.

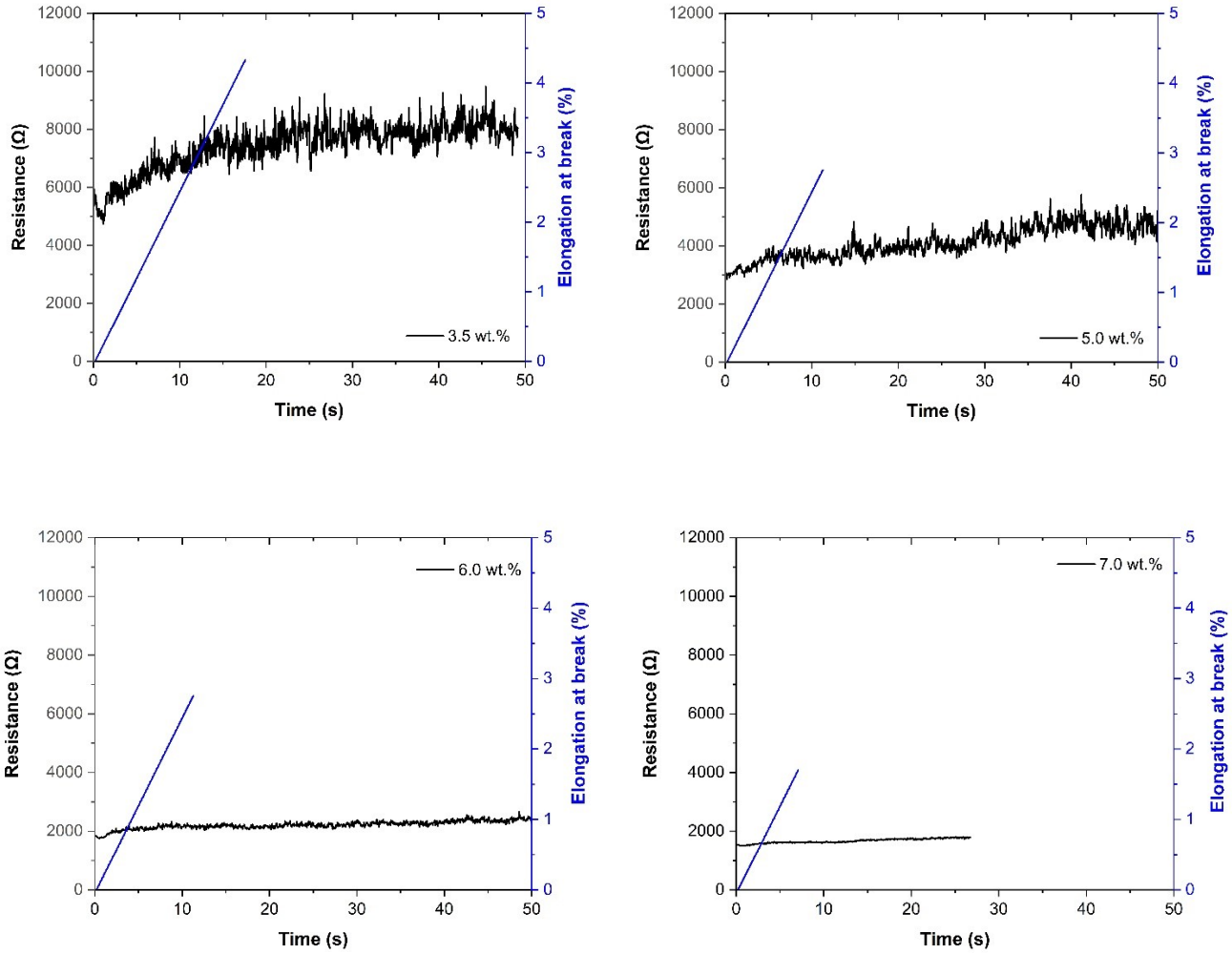

Figure 13. Influence of increasing MWCNT content ((a) 3.5 wt%, (b) 5.0 wt%, (c) 6.0 wt% and (d) 7.0 wt%) of meltspun PEEK-MWCNT monofilament yarns on the absolute change in resistance, during the tensile test to maximum elongation at break.

The electrical and mechanical properties of the melt-spun conductive PEEK-MWCNT monofilamentswith varying MWCNT contents (3.5 wt.%, 5.0 wt.%, 6.0 wt.%, and 7.0 wt.%) were evaluated and compared with CF, as summarized in Table 13. The

comparison allows an assessment of the trade-offs between conductivity, resistivity, and elongation for potential applications of temperatur resistance sensor yarn in structural monitoring. As expected, PEEK-MWCNT monofilaments exhibit considerably lower electrical conductivity than carbon fibers, with maximum σ values reaching ~78 S/m by 7.0 wt.% MWCNT in PEEK compared to 10^4–10^5 S/m for CF. 36–38 Increasing the MWCNT content significantly enhances the electrical conductivity of the PEEK-MWCNT filaments while correspondingly reducing their specific resistivity from 59.9 Ω·mm (3.5 wt.% MWCNT) to 12.8 Ω*mm (7.0 wt.% MWCNT). This trend is accompanied by a decrease in elongation at break from 4.2% to 1.5%, reflecting the typical stiffness and reduced ductility of polymer nanocomposites at high filler loadings. Despite the relatively low conductivity compared to CF, PEEK-MWCNT filaments with 5.0–6.0 wt.% MWCNT maintain sufficient flexibility and elongation (>2.5%) while providing reliable electrical response, making them suitable for incorporation into thermoplastic composite matrices. In contrast, filaments with >6.0 wt.% MWCNT exhibit increased brittleness and limited elongation, which may restrict their application in systems requiring higher strain sensitivity. The mechanical compatibility and residual flexibility of PEEK-MWCNT monofilaments provide a key advantage over brittle carbon fibers, allowing easier processing in thermoplastic composites while still enabling strain- and damage-sensitive sensing. Overall, the PEEK-MWCNT filaments represent a compromise between conductivity and mechanical performance, offering sufficient electrical sensitivity for structural monitoring of thermoplastic composite applications without sacrificing the processability and resilience associated with thermoplastic matrices.

Table 13. Specific Resistivity (ρ), Electrical Conductivity (σ) and Elongation at break of PEEK-MWCNT vs. Carbon Fiber

Material	MWCNT Content (wt.%)	Absolute Resistance R (Ω)	Specific Resistivity ρ (Ω·mm)	Electrical Conductivity σ (S/m)	Elongation at break (%)
PEEK-MWCNT	3.5	7000	59.9	16.7	4.2 ± 0.11
PEEK-MWCNT	5.0	4000	34.3	29.2	2.7 ± 0.10
PEEK-MWCNT	6.0	2000	17.1	58.5	2.5 ± 0.12
PEEK-MWCNT	7.0	1500	12.8	78.1	1.5 ± 0.10
Carbonfiber	–	–	0.01 – 0.1[37]	1×10^4 – 1×10^5 [36]	1.3±0.25

Investigations on PEEK-MWCNT monofilament yarns showed that a pronounced electrical conductivity could only be achieved with an increased MWCNT content (Figure 14). The specific electrical resistance decreased with increasing filler content, which can be attributed to the formation of a conductive network within the polymer matrix. At the same time, however, the increased MWCNT content led to a significant increase in the stiffness of the filaments, which made further textile processing more difficult.

The PEEK-MWCNT monofilament yarns, which were extruded using a ZSE 18 MAXX 40D TSE, had larger filament diameters in the range of 2.5 to 3.5 mm. Based on this, it was assumed that the distribution of MWCNTs within the PEEK matrix is inhomogeneous across the cross-section of the monofilament. To test this hypothesis, the electrical resistance was examined radially along the filament diameter. For this purpose, the monofilaments were mechanically abraded so that both the outer area and the core area were accessible for measurement. The electrical resistance was measured on the surface and in the inner area of the monofilament. The results (Figure 14) showed that the electrical resistance in inside (3225 Ω at 3.5 wt.% MWCNT) was significantly lower than in the outer area (5442 Ω at 3.5 wt.% MWCNT) in all the samples tested. Particularly low resistance values (884 Ω inside and 1378 Ω outside) occurred in samples with a high MWCNT content of 7 wt%, indicating more efficient network formation in the inner region of the filament. Here too, the hypothesis of an inhomogeneous MWCNT distribution across the filament cross-section was assumed. The electrical resistance measurement along the radial diameter was carried out

Textile Science & Research Journal
ISSN: 3059-846X Volume – 1, Issue – 1, 2025
DOI: https://doi.org/10.63456/tsrj-1-1-31

analogously. The results (Figure 14) also confirmed in this case a lower specific electrical resistance in the core area (11.5 Ω*mm ≈ 86.96 S/m) compared to the outer layer (367.7 Ω*mm ≈ 2.72 S/m) of the monofilament. Mokhtari M. et al. 39 showed that they realized semi-conductive PEEK with a low proportion of CNT (< 1 wt.%). Medium to high filler contents (~5-10 wt.%) are required for fully conductive PEEK. This was additionally achieved by adding 10 wt.% of expanded graphite and 10 vol.% of inorganic nickel macroparticles. The electrical conductivity of PEEK was in the conductive range at 1.45 × 10-5 S/m. [39] Gonçalves *et al*. [35] produced PEEK nanocomposite filaments with an electrical conductivity of around 10 S/m, incorporating 4wt.% carbon nanotubes and 3 wt.% graphite nanoplatelets.

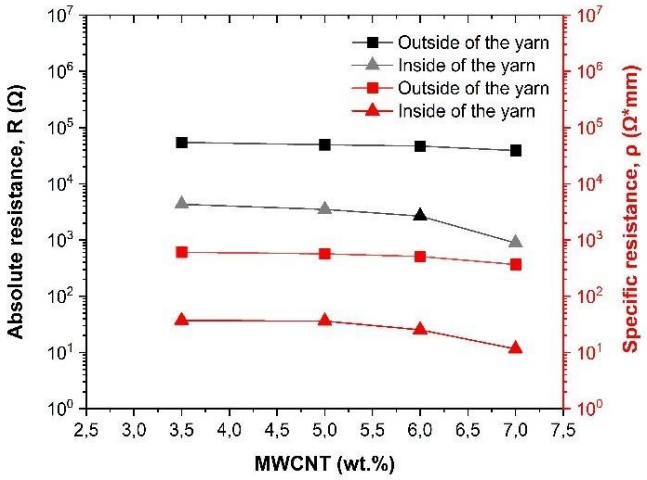

Figure 14. Absolute and specific electrical resistance of the melt-spun PEEK-MWCNT monofilament yarn inside and outside of the monofilament yarn

When analyzing the C-S filament type, consisting of a sheath of PEEK-MWCNT compound and a core of pure PEEK granules, no electrical conductivity could be detected. This indicates that the MWCNT content of 0.5 wt.% used in the core material was not sufficient to form a continuous conductive network. The electrical percolation threshold, which is necessary for the formation of a continuous conductive path, was therefore not reached. The results suggest that a MWCNT content of 3.5 wt.% or more is required to realize electrically conductive structures.

In conclusion, while the absolute conductivity of PEEK-MWCNT monofilaments remains several orders of magnitude below that of CF, the combination of moderate conductivity, improved elongation, and thermoplastic compatibility makes them suitable for SHM applications, where early detection of micro-strains and damage is essential. Above 6.0 wt.% MWCNT, the filaments become brittle and less stretchable, reducing their suitability for flexible composite structures. Compared to brittle CF, PEEK-MWCNT yarns maintain a degree of flexibility and deformation capacity, improving their processability in thermoplastic composites.

CONCLUSIONS

DSC revealed significant effects of MWCNTs on the thermal properties and morphology of semi-crystalline PEEK. The glass transition temperature (Tg) of pure PEEK was measured at 147.17°C, while the addition of 7 wt.% MWCNT increased T_g to 151.80°C (ZSE 18 MAXX 40D), indicating a rise of approximately 5 ± 1°C due to restricted chain mobility from polymer-filler interactions. X_{CF} decreased from 30.61% in pure PEEK to 25.27% at 6 wt.% MWCNT, reflecting the hindrance of polymer chain ordering by MWCNTs. At low filler content (1 wt.% MWCNT), crystallinity slightly increased to 34.08%, demonstrating nucleation promotion. The T_c dropped from 1°C at 1 wt.% MWCNT to 4.5°C at 7 wt.% MWCNT, indicating delayed

crystallization at higher filler concentrations due to MWCNT agglomeration and reduced polymer chain mobility. Melting temperatures remained relatively stable, with pure PEEK melting at 341.54°C and MWCNT-reinforced samples showing a slight decrease to 340.72°C (7 wt.% MWCNT). The X_{RAF} increased from 15.03% in pure PEEK to a maximum of 37.55% at 6 wt.% MWCNT, illustrating enhanced polymer chain immobilization near MWCNT surfaces and optimized interfacial bonding at moderate nanotube concentrations. These findings confirm that while low MWCNT loadings act as nucleating agents enhancing crystallinity and thermal transitions, higher loadings lead to agglomeration effects that hinder crystallization and chain mobility.

Thermogravimetric analysis shows that PEEK exhibits high thermal stability, with initial decomposition starting around 565°C in both oxidative and inert atmospheres. The incorporation of MWCNTs further enhances this stability, as MWCNTs themselves remain intact up to temperatures above 1000°C. In air, PEEK undergoes a two-stage decomposition, while the presence of MWCNTs reduces the mass loss, slows the degradation rate, and improves heat transfer within the material. For composites containing 1 wt.% MWCNTs, the maximum decomposition temperature increases by about 90°C. In nitrogen, PEEK and PEEK–MWCNT composites degrade in a single step and show lower overall mass losses compared to oxidative conditions. Higher MWCNT contents can slightly reduce decomposition temperatures under inert conditions due to the high thermal conductivity of the nanotubes. Overall, the results demonstrate that PEEK–MWCNT composites possess significantly improved thermal stability and are well suited for thermally demanding processes such as melt spinning.

SEM analysis of extruded PEEK/MWCNT filament yarns revealed a clear dependence of microstructure on MWCNT content. At low loadings (1–3.5 wt.%), nanotubes were homogeneously and uniformly dispersed, with almost no large agglomerates, indicating good wetting and efficient dispersion. At higher concentrations (≥5 wt.%), pronounced agglomerates and irregularly distributed clusters were observed due to van der Waals interactions and the limited dispersion capacity of the PEEK matrix. These agglomerates may cause local stress concentrations and negatively affect filament spinnability. Overall, the optimal MWCNT content for uniform dispersion and homogeneous morphology was identified as 1–3.5 wt.%; higher loadings lead to aggregation that could impair mechanical, electrical, and processing properties.

The present study investigates the effects of MWCNT on the processability, mechanical properties and electrical conductivity of MWCNT-based PEEK monofilament yarns and PEEK-MWCNT/PEEK core-sheath filament yarns. By systematically varying the MWCNT concentration (1.0-7.0 wt.%) and the process parameters during extrusion and melt spinning, significant correlations between filler content, process control and resulting material properties were identified. With increasing MWCNT concentration in PEEK, an increase in stiffness (Young's modulus) and tensile strength was observed, but a decrease in elongation at break, indicating embrittlement of the material. Temperatures above 210°C led to increased chain mobility and significantly increased elongation at break (up to 298.9%), but at the expense of mechanical strength. Increasing the yarn draw-off speed led to increased chain orientation and stiffness, but reduced extensibility. The speed of the single-screw extruder for the PEEK sheath component also significantly influenced the mechanical properties and structural homogeneity of the coaxial C-S filament yarns. Higher single-screw extruder speeds improved the centering of the conductive core and led to more homogeneous cross-sectional profiles.

The integration of PEEK/MWCNT–PEEK core–sheath filaments into GF/PP composites maintained or slightly improved mechanical performance compared to the reference composite (Young’s modulus: 11.4 ± 1.45 GPa, tensile strength: 288.99 ± 33.74 MPa, elongation at break: 2.8 ± 0.2%). Optimal processing conditions were identified at a pulloff speed of ~110 m/min with SSE screw speeds of 5–10 rpm, achieving maximum modulus (≈13.1–13.3 GPa) and tensile strength (≈324–338 MPa). Lower pull-off speeds led to slightly reduced stiffness, while excessively high speeds (>120 m/min) caused minor decreases in strength and modulus due to microstructural defects such as voids or partial delamination. These results indicate efficient stress transfer between the sensor yarn and GF/PP matrix and confirm that the conductive PEEK/MWCNT filament can be embedded without compromising composite integrity.

A combination of crimping technique and conductive epoxy adhesive proved to be the most effective method for electrically contacting the sensor-active PEEK-MWCNT filaments, as it significantly reduced the contact resistance and enabled stable measurement results.

The electrical and mechanical characterization of PEEK-MWCNT monofilament yarns revealed a clear tradeoff between conductivity and elongation. Increasing the MWCNT content from 3.5 wt.% to 7.0 wt.% decreased the specific electrical resistance from 59.9 Ω·mm to 12.8 Ω·mm and reduced elongation at break from 4.2% to 1.5%. Low MWCNT contents (3.5–5.0 wt.%) resulted in high resistance (~7000–4000 Ω) and more noise in measurements, while higher contents (6–7 wt.%) achieved lower resistance (~1500 Ω) and stable electrical response. Radial measurements showed inhomogeneous dispersion, with the core area exhibiting lower resistance than the outer layer (e.g., 884 Ω inside vs. 1378 Ω outside at 7 wt.%). Core-sheath filaments with only 0.5 wt.% MWCNT in the core were non-conductive, confirming that ≥3.5 wt.% MWCNT is required to achieve electrical percolation. Overall, PEEK-MWCNT filaments provide moderate conductivity combined with thermoplastic processability and sufficient elongation for structural health monitoring applications, but MWCNT contents above 6.0 wt.% reduce flexibility due to increased brittleness.

CONFLICTS OF INTEREST

The authors declare no conflicts of interest.

ACKNOWLEDGMENTS

The authors disclose that they received financial support for the research, authorship, and/or publication of this article from the German Research Foundation (DFG, Deutsche Forschungsgemeinschaft) under Project ID DFG CH 174/40-2 49 3. The authors thank the German Research Foundation for this support. The authors thank Dr. Iris Kruppke for the translation and linguistic revision of the manuscript. The authors would also like to thank Michael Posselt for conducting the spinning experiments, and Martina Dziewiencka for assisting with the thermogravimetric and differential scanning calorimetry analyses, as well as the SEM measurements.

AUTHOR CONTRIBUTIONS

Toty Onggar: investigation, data curation, visualization, conceptualization, methodology, writing – original draft, formal analysis, resources, funding acquisition. Leopold Alexander Frankenbach: writing – review and editing, formal analysis, funding acquisition. Chokri Cherif: supervision, project manager, writing – review and editing.

DECLARATION OF CONFLICTING INTERESTS

The author(s) declared no potential conflicts of interest with respect to the research, authorship and/or publication of this paper.

FUNDING

This work was supported by Project (ID DFG CH 174/40-249 3) supported by the German Research Foundation (DFG, Deutsche Forschungsgemeinschaft) of German.

DATA AVAILABILITY STATEMENT

The data used to support the findings of this study are included within the article. Further data or information is available from the corresponding author upon request.

REFERENCES

1. Zuo P, Srinivasan DV, Vassilopoulos AP. Review of hybrid composites fatigue. Composite Structures 2021; 274: 114358.
2. Tatar J, Milev S. Durability of Externally Bonded Fiber-Reinforced Polymer Composites in Concrete Structures: A Critical Review. Polymers (Basel) 2021; 13(5): 2–24.
3. Li Y, Chen X, Zhou J, Liu X, Di Zhang, Du F et al. A review of high-velocity impact on fiber-reinforced textile composites: Potential for aero engine applications. Int Journal of Mech Sys Dyn 2022; 2(1): 50–64.
4. Gebrehiwet L, Abate E, Negussie Y, Abeselom E. Application Of Composite Materials In Aerospace & Automotive Industry:Review. International Journal of Advances in Engineering and Management (IJAEM) 2023; 2023(Volume 5, Issue 3):697–723. Available from: URL: file:///d:/user_redir/onggar/Downloads/LijCompositeapplicationarticle.pdf.
5. Saravanan M, Kumar DB. A review on navy ship parts by advanced composite material. Materials Today: Proceedings 2021; 45: 6072–7.
6. Mieloszyk M, Majewska K, Ostachowicz W. Application of embedded fibre Bragg grating sensors for structural health monitoring of complex composite structures for marine applications. Marine Structures 2021; 76: 102903.
7. Baley C, Davies P, Troalen W, Chamley A, Dinham-Price I, Marchandise A et al. Sustainable polymer composite marine structures: Developments and challenges. Progress in Materials Science 2024; 145: 101307.
8. Olhan S, Khatkar V, Behera BK. Review: Textile-based natural fibre-reinforced polymeric composites in automotive lightweighting. J Mater Sci 2021; 56(34): 18867–910.
9. Lakra R, Kumar R, Sahoo PK, Thatoi D, Soam A. A mini-review: Graphene based composites for supercapacitor application. Inorganic Chemistry Communications 2021; 133: 108929.
10. Mishnaevsky L. Sustainable End-of-Life Management of Wind Turbine Blades: Overview of Current and Coming Solutions. Materials (Basel) 2021; 14(5): 1124.
11. Bairagi S, Shahid-ul-Islam, Shahadat M, Mulvihill DM, Ali W. Mechanical energy harvesting and self-powered electronic applications of textile-based piezoelectric nanogenerators: A systematic review. Nano Energy 2023; 111: 108414.
12. Yang CQ, Wang XL, Jiao YJ, Ding YL, Zhang YF, Wu ZS. Linear strain sensing performance of continuous high strength carbon fibre reinforced polymer composites. Composites Part B: Engineering 2016; 102: 86–93.
13. Chen AY, Baehr S, Turner A, Zhang Z, Gu GX. Carbon-fiber reinforced polymer composites: A comparison of manufacturing methods on mechanical properties. International Journal of Lightweight Materials and Manufacture 2021; 4(4): 468–79.
14. Adil S, Lazoglu I. A review on additive manufacturing of carbon fiber-reinforced polymers: Current methods, materials, mechanical properties, applications and challenges. J of Applied Polymer Sci 2023; 140(7): 1-28.
15. Huang X. Fabrication and Properties of Carbon Fibers. Materials (Basel) 2009; 2(4): 2369–403.
16. Cherif C, editor. Textile Werkstoffe für den Leichtbau: Techniken - Verfahren - Materialien - Eigenschaften. Berlin, Heidelberg: Springer; 2011.
17. Chen Y, Hart J, Suh M, Mathur K, Yin R. Electromechanical Characterization of Commercial Conductive Yarns for E-Textiles. Textiles 2023; 3(3): 294–306.
18. Stoppa M, Chiolerio A. Wearable electronics and smart textiles: a critical review. Sensors (Basel) 2014; 14(7): 11957–92.
19. Wang P, Pan A, Xia L, Cao Y, Zhang H, Wu W. Effect of process parameters of fused deposition modeling on mechanical properties of poly-ether-ether-ketone and carbon fiber/poly-ether-ether-ketone. High Performance Polymers 2022; 34(3): 337–51.
20. Ana M. Díez-Pascual, Mohammed Naffakh, Carlos Marco, Gary Ellis, Marián A. Gómez-Fatou. Highperformance nanocomposites based on polyetherketones. Progress in Materials Science 2012 [cited 2025 Jul 9]; (57):1106–90. Available from: URL: https://www.sciencedirect.com/science/article/pii/S0079642512000266.
21. Molinar-Díaz J, Parsons AJ, Ahmed I, Warrior NA, Harper LT. Poly-Ether-Ether-Ketone (PEEK) Biomaterials and Composites: Challenges, Progress, and Opportunities. Polymer Reviews 2025; (65): 527–65.
22. DIN-Normenausschuss Kunststoffe (FNK), Plastics Standards Committee. Plastics - Methods for determining the

density of non-cellular plastics - Part 3: Gas pyknometer method (ISO 1183-3:1999); German version EN ISO 1183-3:1999: BEST Collection 19; Kunststoffindustrie-2025, BEST Collection 21; DIN-Regelwerk-2025, BEST Collection 40; ISO-Exchange-2025, Handbuch Kunststoffe Band 2-2004; 2025 2025 Jun 17. Available from: URL: https://nautos.de/O9G/search/item-detail/DE45801212 [cited 2025 Jul 9].

23. DKE Deutsche Kommission Elektrotechnik Elektronik Informationstechnik in DIN und VDE, German Commission for Electrical, Electronic and Information Technologies of DIN and VDE. Dielectric and resistive properties of solid insulating materials - Part 2-3: Relative permittivity and dissipation factor - Contact electrode method for insulating films - AC methods (IEC 62631-2-3:2024); German version EN IEC 62631-2-3:2024: DIN Deutsches Institut für Normung e. V., DIN German Institute for Standardization; 2025 2025 Jun 17. Available from: URL: https://nautos.de/O9G/search/item-detail/DE30104946 [cited 2025 Jul 9].
24. D20 Committee. Test Method for Transition Temperatures and Enthalpies of Fusion and Crystallization of Polymers by Differential Scanning Calorimetry. West Conshohocken, PA: ASTM International.
25. Silva S, Barbosa JM, Sousa JD, Paiva MC, Teixeira PF. High-Performance PEEK/MWCNT Nanocomposites: Combining Enhanced Electrical Conductivity and Nanotube Dispersion. Polymers (Basel) 2024; 16(5): 583.
26. Dydek K, Latko-Durałek P, Sulowska A, Kubiś M, Demski S, Kozera P et al. Effect of Processing Temperature and the Content of Carbon Nanotubes on the Properties of Nanocomposites Based on Polyphenylene Sulfide. Polymers (Basel) 2021; 13(21): 3816.
27. Awaja F, Zhang S. Self-bonding of PEEK for active medical implants applications. J. of Adhesion Science and Technology, 2015; 29(15): 1593-1606.
28. Gohn AM, Seo J, Colby RH, Schaake RP, Androsch R, Rhoades AM. Crystal nucleation in poly(ether ether ketone)/carbon nanotube nanocomposites at high and low supercooling of the melt; Polymer, 2020; 199; 122548.
29. Rinaldi M, Ghidini T, Nanni F. Fused filament fabrication of polyetheretherketone/multiwalled carbon nanotube nanocomposites: the effect of thermally conductive nanometric filler on the printability and related properties. Polymer International 2021; 70(8): 1080–9.
30. Kayginok F, Karabal M, Yıldız A, Cebeci H. CNT reinforced PEI and PEEK nanocomposites: A comparison on the thermal and rheological properties. Polymer Testing 2024; 137: 108519.
31. Shang Y, Wu X, Liu Y, Jiang Z, Wang Z, Jiang Z et al. Preparation of PEEK/MWCNTs composites with excellent mechanical and tribological properties. High Performance Polymers 2019; 31(1): 43–50.
32. Feng S, Liu C, Sue H-J. Preparation of PEEK/MWCNT nanocomposites via MWCNT-induced interfacial crystallization mediated compatibilization. Composites Science and Technology 2022; 221: 109298.
33. Ma R, Zhu B, Zeng Q, Wang P, Wang Y, Liu C et al. Melt-Processed Poly(Ether Ether Ketone)/Carbon Nanotubes/Montmorillonite Nanocomposites with Enhanced Mechanical and Thermomechanical Properties. Materials (Basel) 2019; 12(3): 525.
34. Shokrieh, M M, Saeedi, Ali, Chitsazzadeh, Majid. Mechanical properties of multi-walled carbon nanotube/polyester nanocomposites - Journal of Nanostructure in Chemistry 2013; 3(20): 1-5. Available from: URL: https://link.springer.com/article/10.1186/2193-8865-3-20.
35. Gonçalves J, Lima P, Krause B, Pötschke P, Lafont U, Gomes JR et al. Electrically Conductive Polyetheretherketone Nanocomposite Filaments: From Production to Fused Deposition Modeling. Polymers (Basel) 2018; 10(8): 925.
36. Zhao Q, Zhang K, Zhu S, Xu H, Cao D, Zhao L et al. Review on the Electrical Resistance/Conductivity of Carbon Fiber Reinforced Polymer. Appl. Sci. 2019; 9(11): 2390.
37. Wang X, Fu X, Chung DDL. Strain sensing using carbon fiber. J of Materiala Research. 2011; 14: 790-802.
38. Supreem Carbon. carbon-fiber-electrical-conductivity-essential-guide-for-industry; 2025 [cited 2025 Nov 4]. Available from: URL: https://www.supreemcarbon.com/article/carbon-fiber-electrical-conductivity-essentialguide-for-industry.html.
39. Mokhtari M, Archer E, Bloomfield N. A review of electrically conductive poly(ether ether ketone) materials. Polymer International 2021; (70): 1016–25.